bioRxiv preprint doi: https://doi.org/10.1101/2023.05.05.539519; this version posted May 5, 2023. The copyright holder for this preprint (which was not certified by peer review) is the author/funder, who has granted bioRxiv a license to display the preprint in perpetuity. It is made available under aCC-BY 4.0 International license.

# Title: ADARs employ a neural-specific mechanism to regulate PQM-1 expression and survival from hypoxia

**Short Title:** ADAR-mediated gene regulation affects hypoxia survival

Ananya Mahapatra[1], Alfa Dhakal[2], Aika Noguchi[3], Pranathi Vadlamani[4], Heather A. Hundley[3*]

1. Genome, Cell and Developmental Biology Graduate Program, Indiana University, Bloomington IN, 47405 USA
2. Cell, Molecular and Cancer Biology Graduate Program, Indiana University School of Medicine – Bloomington, Bloomington IN, 47405 USA
3. Department of Biology, Indiana University, Bloomington IN 47405 USA
4. Medical Sciences Program, Indiana University School of Medicine – Bloomington, Bloomington IN, 47405 USA

* corresponding author – email: hahundle@indiana.edu

## Abstract

The ability to alter gene expression programs in response to changes in environmental conditions is central to the ability of an organism to thrive. For most organisms, the nervous system serves as the master regulator in communicating information about the animal's surroundings to other tissues. The information relay centers on signaling pathways that cue transcription factors in a given cell type to execute a specific gene expression program, but also provide a means to signal between tissues. The transcription factor PQM-1 is an important mediator of the insulin signaling pathway contributing to longevity and the stress response as well as impacting survival from hypoxia. Herein, we reveal a novel mechanism for regulating PQM-1 expression specifically in neural cells of larval animals. Our studies reveal that the RNA binding protein, ADR-1, binds to *pqm-1* mRNA in neural cells. This binding is regulated by the presence of a second RNA binding protein, ADR-2, which when absent leads to reduced expression of both *pqm-1* and downstream PQM-1 activated genes. Interestingly, we find that neural *pqm-1* expression is sufficient to impact gene expression throughout the animal and affect survival from hypoxia; phenotypes that we also observe in *adr* mutant animals. Together, these studies reveal an important post-transcriptional gene regulatory mechanism that allows the nervous system to sense and respond to environmental conditions to promote organismal survival from hypoxia.

bioRxiv preprint doi: https://doi.org/10.1101/2023.05.05.539519; this version posted May 5, 2023. The copyright holder for this preprint (which was not certified by peer review) is the author/funder, who has granted bioRxiv a license to display the preprint in perpetuity. It is made available under aCC-BY 4.0 International license.

## Introduction

Aerobic heterotrophs need to obtain nutrition and oxygen from the environment, the prolonged absence of which can lead to undesirable consequences including death. However, fluctuations in oxygen and nutrient availability are common in nature and during development; thus, organisms must have a means to both sense the environment and respond. At the most extreme, animals can effectively halt developmental and cellular programs resulting in a transient quiescent state [1]. For example, in the model organism *Caenorhabditis elegans* (*C. elegans*), the absence of oxygen can lead to a state of "suspended animation" [2], while first larval stage (L1) animals hatched in the absence of food enter a state of halted development commonly referred to as "L1 arrest" [3, 4].

An animal's ability to enact these responses relies on the presence of a nervous system that can translate environmental information into physiological responses [5]. Neural gene expression programs are critical for organismal survival to many stresses. However, the nervous system must also communicate information about the environment to other tissues to promote diverse outputs, including behaviors and metabolic changes needed for organismal survival [6-8]. This trans-tissue communication is difficult to study in humans, but, altered brain-gut communication has been implicated in both oncogenesis and neurodegenerative diseases [9, 10]. In contrast, studies in model organisms have been instrumental in demonstrating that the nervous system signals to the peripheral tissues to promote survival and longevity in response to stress [11]. Furthermore, recent data indicates that not only do some peripheral tissues receive the stress signals from the nervous system, but tissues like the intestine can also serve as an important regulatory organ, sending signals back to the nervous system to promote health and longevity [12].

The molecular players underlying the response to environmental conditions are conserved signaling pathways. The major signaling pathways that respond to nutrients include the AMP-activated protein kinase and Target of Rapamycin pathways, while the Hypoxia-inducible factor 1 pathway responds to low oxygen (hypoxia) [13, 14]. In addition, there is cross-talk between the insulin signaling pathway and all of these pathways [14-16], thereby making insulin signaling a key determinant of how animals respond to diet and environmental fluctuations in oxygen levels. In *C. elegans*, the insulin signaling pathway has only one known receptor, DAF-2, which is homologous to both the mammalian insulin receptor and insulin-like growth factor 1 receptor [17]. Despite having only one receptor, there are over 40 insulin-like peptides (ILPs) encoded in the *C. elegans* genome [18]. Binding to these agonists and antagonists can influence the ability of DAF-2 to signal to downstream kinases that in turn regulate at least two transcription factors, the well-established FOXO homolog DAF-16 and/or the more recently identified zinc finger protein PQM-1 [19, 20].

Genetic dissection of the insulin signaling pathway, particularly the study of temperature-sensitive loss of function mutations of *daf-2*, has identified a central role for this pathway in regulating development, longevity, metabolism and reproduction [19, 21, 22]. In addition to genomic mutations, which impact signaling throughout the animal, it is well established that the nervous system is the critical site of action for insulin signaling to regulate diverse aspects of *C. elegans* physiology [23]. For example, neuronal-

bioRxiv preprint doi: https://doi.org/10.1101/2023.05.05.539519; this version posted May 5, 2023. The copyright holder for this preprint (which was not certified by peer review) is the author/funder, who has granted bioRxiv a license to display the preprint in perpetuity. It is made available under aCC-BY 4.0 International license.

specific expression of the insulin receptor rescues both the long-lived phenotype observed in adult animals with altered DAF-2 function as well as the formation of dauer larva, a developmentally arrested life stage that is induced by over-crowding and starvation in wildtype *C. elegans* but constitutively occurs in *daf-2* mutant larval animals [24, 25]. Recently a novel regulatory mechanism for altering insulin signaling via alternative splicing of *daf-2* in neurons was identified [26]. The resulting DAF-2B protein retains the extracellular domain but lacks the intracellular domains to mediate downstream signaling, which allows the DAF-2B protein to bind ILPs and influence insulin signaling by competing with full-length DAF-2. Consistent with this, the presence of DAF-2B influences dauer entry and recovery as well as lifespan, further supporting the idea that nervous system-specific regulation of the insulin signaling pathway is important.

Previous studies from our lab identified adenosine (A) to inosine (I) RNA editing sites in *daf-2* mRNA isolated from neural cells of L1-arrested animals [27]. Due to differences in base-pairing properties of adenosine and inosine, A-to-I editing events can impact gene expression depending on the region of RNA in which the editing event occurs [28, 29]. For example, A-to-I editing within coding sequences of genes can alter the protein encoded by the gene and editing within 3' untranslated regions (UTRs) can alter small RNA binding [30]. For the *daf-2* transcript, the A-to-I editing sites identified are located within an intronic sequence, which could potentially impact the production of *daf-2* splice isoforms. To begin to understand if RNA editing influences DAF-2 function, we examined gene expression changes that occur in neural cells in the absence of the enzyme that is responsible for catalyzing the hydrolytic deamination of adenosine to inosine, ADR-2. ADR-2 is a member of the adenosine deaminase that act on RNA (ADAR) family, and the *C. elegans* genome encodes two ADAR family members ADR-1 and ADR-2 [31]. ADR-2 is the sole A-to-I editing enzyme in *C. elegans* [32, 33], as ADR-1 lacks essential amino acids required to perform deamination [32]. However, as ADARs are RNA binding proteins (RBPs) that can also regulate gene expression through binding RNA [34], both ADR-1 and ADR-2 may play roles in editing-independent gene regulation in *C. elegans*. Interestingly, the long-lived phenotype of animals lacking *daf-2* is also observed in *adr-2(-)* mutants [24, 35]. Together, these data suggested the possibility of *C. elegans* ADARs impacting insulin signaling. While a role for ADARs in regulating insulin signaling is relatively unexplored, recent work in β cells indicated that the pathophysiological environment of type 1 diabetes patients influences RNA editing [36]. In this work, we sought to determine how ADARs can affect the insulin signaling pathway, particularly in the nervous system of L1-arrested *C. elegans*.

## Results

### *Decreased expression of genes regulated by insulin signaling upon loss of adr-2*

As a first step towards addressing whether ADR-2 regulates insulin signaling, the transcriptomes of wildtype and *adr-2* deficient animals were compared. As editing of *daf-2* was observed in neural cells isolated from synchronized L1 animals [27], differential gene expression was analyzed in RNA isolated from these same types of biological samples. Using datasets from previously performed RNA-sequencing (RNA-

bioRxiv preprint doi: https://doi.org/10.1101/2023.05.05.539519; this version posted May 5, 2023. The copyright holder for this preprint (which was not certified by peer review) is the author/funder, who has granted bioRxiv a license to display the preprint in perpetuity. It is made available under aCC-BY 4.0 International license.

seq) of three biological replicates of wildtype and *adr-2(-)* neural cells from synchronized L1 animals [37], differential gene expression analysis identified 697 genes significantly altered in neural cells from *adr-2(-)* animals ($p$ value < 0.05 and $\log_2$fold change > |0.5|), with nearly three times as many downregulated genes (501) as upregulated genes (196) (Figure 1A, Supplemental Table S1). These misregulated genes were subjected to gene set enrichment analysis using a *C. elegans* specific software, WormCat [38]. The analysis for genes upregulated in neural cells from *adr-2(-)* animals revealed only one significantly enriched gene set, extracellular material (Supplemental Figure S1). The downregulated genes were enriched for four gene sets: stress response, proteolysis, metabolism and lysosome (Supplemental Figure S1). As DAF-2-mediated signaling regulates both stress response and metabolism [19], this suggests that loss of *adr-2* might result in altered insulin signaling in neural cells. However, it should be noted that we did not observe significant changes in *daf-2* mRNA expression in *adr-2(-)* neural cells (Supplemental Table S1).

To independently examine the expression of genes regulated by DAF-2, qPCR was performed for three known downstream targets in three independent biological replicates of neural cells isolated from wildtype and *adr-2(-)* animals. Consistent with the RNA-seq dataset, all three genes (*dod-17*, *dod-19*, and *dod-24*) examined were significantly downregulated in *adr-2(-)* neural cells compared to wildtype neural cells (Figure 1B). These results suggest that, within neural cells, there is decreased expression of genes regulated by DAF-2 upon loss of *adr-2*.

While this data suggests that loss of *adr-2* affects genes regulated by insulin signaling in the nervous system, the nervous system is also the master regulator that coordinates gene regulation between tissues [39]. Studies have demonstrated that DAF-2 function in the nervous system can affect phenotypes such as organismal lifespan by signaling to other tissues [25]. This raised the question of whether the decreased expression of DAF-2-regulated genes upon *adr-2* loss could be observed in RNA isolated from whole L1 animals. Furthermore, the neural cells were isolated from L1 animals that were synchronized by hatching in the absence of food, and nutrient levels impact insulin signaling [40]. Hence, gene expression was examined in RNA isolated from three independent biological replicates of synchronized wildtype and *adr-2(-)* L1 animals as well as a subset of these hatched L1 animals that were exposed to bacterial food for six hours. Similar to neural cells, all three genes (*dod-17*, *dod-19*, and *dod-24*) exhibited significantly decreased expression in hatched L1 animals lacking *adr-2* compared to wildtype animals (Figure 1C). This suggests that the impacts of loss of *adr-2* on altered neural gene expression (Figure 1A, B) may lead to cell non-autonomous effects and/or that *adr-2* regulates genes downstream of insulin signaling in several tissues. In contrast to the hatched L1 animals, there was no significant difference in expression of the three genes (*dod-17*, *dod-19*, and *dod-24*) between wildtype and *adr-2(-)* animals after feeding for six hours (Figure 1C).

Together these data suggest that upon loss of *adr*-2, reduced expression of genes regulated by insulin signaling occurs in whole animals and is abrogated by the presence of food. Since the observed decreased gene expression was specific to starved *adr-2(-)* animals and insulin signaling is known to impact starvation responses in *C. elegans*, these data suggested that *adr-2* regulates *dod-17*, *dod-19*, and *dod-24* through the insulin signaling pathway. To directly test this possibility, genetic mutants of

bioRxiv preprint doi: https://doi.org/10.1101/2023.05.05.539519; this version posted May 5, 2023. The copyright holder for this preprint (which was not certified by peer review) is the author/funder, who has granted bioRxiv a license to display the preprint in perpetuity. It is made available under aCC-BY 4.0 International license.

*adr-2* and *daf-2* [41] were combined and gene expression was examined. As observed consistently in this study, compared to wildtype animals, *dod-17*, *dod-19*, and *dod-24* were all significantly reduced in *adr-2(-)* animals (Figure 1D). Consistent with previous studies [42], *dod-17*, *dod-19*, and *dod-24* all exhibited significantly decreased expression in *daf-2(-)* animals (Figure 1D). Compared to wildtype animals, there was a significant reduction in mRNA expression of all three insulin signaling regulated genes in the *adr-2(-);daf-2(-)* double mutants (Figure 1D). Additionally, the expression profile of *dod-17*, *dod-19*, and *dod-24* was similar between the *adr-2(-)* and *daf-2(-)* single mutants and the *adr-2(-);daf-2(-)* double mutants (Figure 1D). Together, these data indicate that lack of *adr-2* leads to decreased expression of insulin signaling regulated genes and the regulation occurs through the DAF-2 pathway.

### *Regulation of insulin signaling by ADR-2 is cell non-autonomous and editing-independent*

In addition to being expressed in the nervous system, genes regulated by insulin signaling are also highly expressed in the intestine [43, 44]. As the RNA isolated from L1 animals hatched in the absence of food shows decreased gene expression similar to neural cells, this suggests that loss of *adr-2* can potentially result in altered insulin-signaling in both neural and intestinal cells. However, there is extensive communication between neural cells and the intestine; thus, it is possible that loss of *adr-2* in neural cells is sufficient to result in altered insulin signaling in the intestine. To test this possibility, gene expression was monitored in animals that express ADR-2 only in the nervous system [37]. Briefly, these transgenic animals were generated by injecting *adr-2(-)* animals with a plasmid construct in which a pan-neural promoter *rab-3* drives the expression of *adr-2* along with a co-injection marker expressing GFP. A similar strain was previously generated by our lab and shown to result in ADR-2 activity in the nervous system [37]. Since transgenes do not exhibit 100% inheritance in *C. elegans,* the transgenic animals of interest were sorted for GFP expression using the COPAS Select large particle sorter. Optimized COPAS conditions in terms of extinction and time of flight were used to create a gated window for specifically sorting L1 animals. RNA was isolated from the sorted animals and qPCR was performed to assess gene expression. It was observed that compared to *adr-2* lacking animals, animals expressing ADR-2 solely in the nervous system significantly rescued expression of genes regulated by insulin signaling (Figure 2A). This data suggests that the presence of ADR-2 in the nervous system regulates insulin signaling throughout the animals.

To further validate that neural ADR-2 regulates insulin signaling regulated genes throughout the animal, confocal microscopy was performed to monitor expression of one of these genes, *dod-24*, upon loss of *adr-2* in whole animals. Synchronized L1 animals expressing GFP driven by the *dod-24* promoter [43] were analyzed. In wildtype animals, transcription from the *dod-24* promoter was observed in neural as well as intestinal cells as expected [43] (Figure 2B). Upon loss of *adr-2,* decreased GFP expression was observed throughout the animal (Figure 2B), which is consistent with the qPCR analysis of *dod-24* expression (Figure 1C). Furthermore, in animals expressing ADR-2 solely in the nervous system, GFP expression was similar to wildtype

bioRxiv preprint doi: https://doi.org/10.1101/2023.05.05.539519; this version posted May 5, 2023. The copyright holder for this preprint (which was not certified by peer review) is the author/funder, who has granted bioRxiv a license to display the preprint in perpetuity. It is made available under aCC-BY 4.0 International license.

animals (Figure 2B). These results demonstrate that the presence of ADR-2 in the nervous system cell non-autonomously impacts gene expression.

To begin to dissect the molecular function of ADR-2 in the nervous system that contributed to the altered gene regulation, expression of *dod-17*, *dod-19*, and *dod-24* was examined in animals expressing an ADR-2 mutant (ADR-2 G184R) that can bind RNA, but lacks the ability to edit [27]. As observed consistently in this study, hatched L1 *adr-2(-)* animals had significantly decreased expression of insulin signaling regulated genes compared to wildtype animals (Figure 2C). In contrast, gene expression in the ADR-2 G184R animals was similar to wildtype animals (Figure 2C). Together, these results indicate that, while the presence of ADR-2 in the nervous system is critical for proper *dod-17*, *dod-19*, and *dod-24* expression throughout the animal, the editing function of ADR-2 is not required for this gene regulatory function.

### *Neural pqm-1 levels impact downstream gene expression throughout the animal*

As the ADR-2 editing function was not required for altered *dod-17*, *dod-19*, and *dod*-24 expression, editing of *daf-2* is unlikely to be causing the decreased expression of downstream insulin signaling regulated genes in neural cells and animals lacking *adr-2*. As DAF-2 is at the top of the insulin-signaling regulatory cascade and transcriptional output is mediated by at least two different transcription factors, DAF-16 and PQM-1, we sought to examine whether all DAF-2 regulated genes were equally affected by loss of *adr-2*. The up- and downregulated genes in the *adr-2(-)* neural RNA-seq dataset were individually overlapped with either DAF-16 activated or PQM-1 activated genes from a published dataset [20] (Supplemental Figure S2). The number of PQM-1 activated genes that were downregulated in *adr-2(-)* neural cells (156) was nearly three times the number that would be expected by random chance (53) (Supplemental Figure S2) and *dod-17*, *dod-19* and *dod-24* are all genes activated by PQM-1 [20]. The number of overlapping PQM-1 activated genes that were upregulated in *adr-2(-)* neural cells (11) was lesser than that obtained due to random chance (20) (Supplemental Figure S2). Further, the number of overlapping DAF-16 activated genes either up- (23) or downregulated (61) in *adr-2(-)* neural cells was very close to what would be expected from random chance (Supplemental Figure S2). These results suggest that loss of *adr-2* does not impact all genes downstream of the insulin signaling pathway, but instead, leads to specific downregulation of PQM-1-activated genes.

The above data raised the question of whether loss of *adr-2* directly impacts *pqm-1* expression. To address this question, *pqm-1* expression was monitored in both neural cells and L1 animals using qPCR. In the neural cells from *adr-2(-)* animals, there was a significant decrease in *pqm-1* expression compared to neural cells isolated from wildtype animals (Figure 3A). Consistent with this finding, our neural RNA-seq datasets also revealed that loss of *adr-2* indeed resulted in significantly decreased neural expression of *pqm-1* (Supplemental Table S1). In contrast to neural cells, *pqm-1* expression was not significantly altered in RNA isolated from synchronized L1 animals lacking *adr-2* (Figure 3B). Together, this data indicates that the lack of *adr-2* impacts *pqm-1* expression in a tissue-specific manner. The data also suggests that decreased neural expression of *pqm-1* upon loss of *adr-2* could impact gene expression throughout the animal.

bioRxiv preprint doi: https://doi.org/10.1101/2023.05.05.539519; this version posted May 5, 2023. The copyright holder for this preprint (which was not certified by peer review) is the author/funder, who has granted bioRxiv a license to display the preprint in perpetuity. It is made available under aCC-BY 4.0 International license.

To directly address whether the decreased expression of PQM-1-activated genes in *adr-2(-)* animals is due to decreased *pqm-1* expression, gene expression was assessed in animals lacking *pqm-1(-)* and *adr-2(-);pqm-1(-)* animals. Briefly, *pqm-1(ok485)* animals [45] were obtained and backcrossed to wildtype animals before crossing to *adr-2(-)* animals. RNA was then isolated from wildtype, *adr-2(-)*, *pqm-1(-)* and *adr-2(-)*;*pqm-1(-)* animals obtained from the genetic cross. As expected, compared to wildtype animals, *adr-2(-)* animals showed significantly decreased expression of *dod-17*, *dod-19* and *dod-24* (Figure 3C). Similarly, loss of *pqm-1* resulted in significantly decreased expression of *dod-17*, *dod-19* and *dod-24* compared to wildtype animals (Figure 3C). These PQM-1 activated genes also showed a significant reduction in expression in *adr-2(-);pqm-1(-)* animals (Figure 3C), which was similar to the expression levels observed in the individual *adr-2(-)* and *pqm-1(-)* mutant animals (Figure 3C). These results suggest that the decreased expression of *dod-17*, *dod-19* and *dod-24* upon loss of *adr-2* occurs via altered PQM-1 function.

As our results clearly indicate that loss of *adr-2* leads to downregulation of *pqm-1* specifically in the nervous system, but decreased expression of PQM-1 activated genes throughout L1 animals, we sought to test whether expressing *pqm-1* only within the nervous system of *adr-2(-)* animals could restore *dod-17*, *dod-19* and *dod-24* gene expression in L1 animals. Transgenic animals were generated by injecting a plasmid in which *pqm-1* expression is driven by the neuronal *rab-3* promoter. As a control, this plasmid was first injected into *pqm-1(-)* animals to observe gene expression changes in *pqm-1(-)* animals. The resulting transgenic animals were crossed with *adr-2(-)* animals and genotyped for either *pqm-1(-)* or *adr-2(-)* animals that specifically express *pqm-1* in the nervous system. Compared to wildtype animals and consistent with other results in this study, there was significantly decreased expression of *dod-17*, *dod-19* and *dod-24* in *pqm-1(-)* animals (Figure 3D). However, *pqm-1(-)* animals expressing *pqm-1* only in the nervous system had significantly increased expression of *dod-17*, *dod-19* and *dod-24*, which rescued the gene expression to near wildtype levels (Figure 3D). As observed throughout this study, *adr-2(-)* animals exhibited significantly decreased expression of PQM-1 activated genes compared to wildtype animals (Figure 3D). However, *adr-2(-)* animals carrying the neural *pqm-1* transgene exhibited significantly increased expression of *dod-17*, *dod-19* and *dod-24* compared to animals lacking *adr-2* (Figure 3D). Together, these data indicate that lack of *adr-2* leads to global downregulation of *dod-17*, *dod-19* and *dod-24* via decreased expression of the PQM-1 transcription factor in the nervous system.

### *In the absence of adr-2, ADR-1 binds to pqm-1 mRNA and results in decreased expression of PQM-1 activated genes*

The above data suggest that loss of *adr-2* results in decreased *pqm-1* expression in the nervous system, which leads to decreased expression of PQM-1 activated genes throughout the animal. Since the editing function of ADR-2 is not required for the downregulation of these PQM-1 activated genes (Figure 2C), we sought to test what other function of ADR-2 was critical for regulating *pqm-1* expression. ADR-2 directly interacts with ADR-1, a deaminase-deficient member of the ADAR family present in *C. elegans* [46]. The physical interaction between ADR-1 and ADR-2 can both promote

bioRxiv preprint doi: https://doi.org/10.1101/2023.05.05.539519; this version posted May 5, 2023. The copyright holder for this preprint (which was not certified by peer review) is the author/funder, who has granted bioRxiv a license to display the preprint in perpetuity. It is made available under aCC-BY 4.0 International license.

ADR-2 binding to RNA [46], as well as influence the RNAs that ADR-1 binds [35]. However, the biological impacts of this latter function are relatively unknown. To assess if PQM-1 activation of gene expression is altered upon loss of *adr-1*, RNA was isolated from hatched wildtype, *adr-1(-)*, *adr-2(-)* and *adr-1(-)*;*adr-2(-)* L1 animals, and qPCR was performed to measure gene expression of *dod-17*, *dod-19* and *dod-24* in these animals. Consistent with the data obtained in this study, *adr-2(-)* animals had decreased expression of the PQM-1 activated genes compared to wildtype animals (Figure 4A). In contrast, expression levels of *dod-17*, *dod-19* and *dod-24* were similar between wildtype and *adr-1(-)* animals (Figure 4A), suggesting that loss of ADR-1 function did not affect PQM-1-mediated gene regulation in wildtype animals. Interestingly, loss of *adr-1* in animals lacking *adr-2* significantly increased expression of PQM-1 activated genes compared to animals lacking only *adr-2* (Figure 4A). These results suggest that ADR-1 has a unique function in the absence of *adr-2*, which results in decreased expression of PQM-1 activated genes.

So far, the data suggests that upon loss of *adr-2,* decreased *pqm-1* expression in neural cells leads to global downregulation of PQM-1 activated genes and loss of *adr-1* can rescue these downstream gene expression changes. As ADR-1 is an RNA binding protein, we sought to determine whether ADR-1 directly binds *pqm-1* mRNA specifically in the nervous system, and whether that binding is influenced by the presence or absence of *adr-2*. To examine binding of ADR-1 to *pqm-1* in the L1 nervous system, an RNA immunoprecipitation (RIP) assay was performed with animals that express ADR-1 specifically in the nervous system. To generate these animals *adr-1(-)* animals were injected with a construct in which the neuronal *rab-3* promoter drives expression of an N-terminally 3X FLAG *adr-1* genomic sequence. A similar epitope tagged construct under the control of the *adr-1* endogenous promoter was previously demonstrated to produce functional ADR-1 protein [33]. Hatched L1 animals were subjected to UV crosslinking to stabilize RNA-protein interactions prior to generation of protein lysates. ADR-1 and associated bound RNAs were immunoprecipitated using magnetic FLAG beads. ADR-1 was efficiently immunoprecipitated from animals expressing ADR-1 in the nervous system both in the presence and absence of *adr-2*, but not from lysates of the negative control *adr-1(-)* animals (Figure 4B). On assessing *pqm-1* mRNA in the assay, compared to the negative control, there was no enrichment for *pqm-1* mRNA in IPs from neural ADR-1-expressing animals that expressed wildtype ADR-2 (Figure 4B). However, a 5-fold enrichment of *pqm-1* mRNA was observed in the neural ADR-1 RIP in the absence of *adr-2* (Figure 4B). This data suggests that *in vivo,* ADR-1 binds *pqm-1* in the nervous system, but only in the absence of *adr-2*.

To further examine whether the RNA binding function of ADR-1 is contributing to the decreased expression of PQM-1 activated genes observed in *adr-2(-)* animals, *dod-17*, *dod-19* and *dod-24* expression was monitored in *adr-2* lacking animals that also have abolished ADR-1 binding. These mutant animals have three mutations within the conserved KKxxK motif (where K is lysine and x is any amino acid) of the first dsRNA binding domain (dsRBD1) of ADR-1 (K223E, K224A, K227A), which was previously shown to disrupt the ability of ADR-1 to bind RNA *in vivo* [46]. The mutation was introduced in wildtype animals with an integrated 3X FLAG tag at the *adr-1* locus via CRISPR by using a guide RNA targeted to the *adr-1* locus and a HDR template containing the desired mutations. These animals were then crossed to *adr-2(-)* animals

bioRxiv preprint doi: https://doi.org/10.1101/2023.05.05.539519; this version posted May 5, 2023. The copyright holder for this preprint (which was not certified by peer review) is the author/funder, who has granted bioRxiv a license to display the preprint in perpetuity. It is made available under aCC-BY 4.0 International license.

to generate *adr-2(-)* animals that also lack the ADR-1 binding function. RNA was isolated from these animals as well as wildtype and *adr-2(-)* animals and qPCR was performed. Compared to *adr-2(-)* animals, *adr-2(-);* ADR-1 dsRBD1 mutants had significantly increased expression of *dod-17*, *dod-19* and *dod-24* (Figure 4C). Together, these results indicate that in the absence of *adr-2,* ADR-1 binds *pqm-1* in the nervous system, which leads to decreased expression of PQM-1 activated genes throughout the animal.

### *PQM-1 functions in the nervous system to regulate hypoxia survival of L1-arrested animals*

Previous studies have indicated that PQM-1 is a negative regulator of hypoxic survival in fourth stage larval (L4) animals [47]. As our data indicates that *adr-2(-)* animals have decreased *pqm-1* expression, we sought to determine if these animals also had altered survival to hypoxic exposure. Additionally, since the data so far indicate that ADARs regulate *pqm-1* expression specifically in the nervous system, whether neural PQM-1 specifically plays a role in survival to hypoxia was of interest.

To directly test these questions, hatched L1 animals were exposed to varying concentrations of cobalt chloride ($CoCl_2$), which serves as a hypoxia mimetic [48]. As we wanted to address the contribution of neural PQM-1 in regulating hypoxia, survival of the neural-specific *pqm-1* transgenic animals was examined. However, as the neural *pqm-1* strains were transgenic, to avoid any non-specific effects of the coinjected transgenes, survival was compared in animals that all carry the *prab-3::*GFP transgene. Wildtype, *pqm-1(-)*, *pqm-1(-)* animals expressing *pqm-1* in the nervous system*, adr-2(-)* and *adr-2(-)* animals overexpressing *pqm-1* in the nervous system were used in the hypoxic survival experiment. After obtaining hatched L1 animals, 5000 animals per strain were washed with NaCl and then exposed to varying concentrations of $CoCl_2$ (0 - 80 mM) for two hours. After the $CoCl_2$ exposure, three technical replicates of GFP positive 30-40 L1 animals per strain were plated and incubated for twenty-four hours at 20°C in the presence of food. To measure hypoxic survival, alive and dead animals were counted for all the strains and plotted for all concentrations of $CoCl_2$. At lower concentrations of $CoCl_2$ (2.5 mM and 5 mM), the number of alive L1s was similar across all worm strains (Figure 5A). However, at 10 mM and higher concentrations of $CoCl_2$, consistent with previous studies [49], there was a drastic reduction in the survival of wildtype animals (Figure 5A). With increasing concentrations of $CoCl_2$, the number of alive *pqm-1(-)* and *adr-2(-)* animals was significantly higher than wildtype animals (Figure 5A, Supplemental Figure S3), suggesting an increased hypoxic survival of these animals. Strikingly, there was a sharp decline in the survival of *pqm-1(-)* animals expressing neural *pqm-1* compared to *pqm-1(-)* animals (Figure 5A, Supplemental Figure S3). This data suggests that PQM-1 function within the nervous system is sufficient to regulate hypoxic survival. Interestingly, a similar result was observed with *adr-2(-)* animals with transgenic expression of *pqm-1* in the nervous system (Figure 5A, Supplemental Figure S3). Together, these data suggest that PQM-1 in the nervous system is a critical regulator of hypoxia survival in hatched L1 animals and that this function of PQM-1 impacts the survival of animals lacking *adr-2* in hypoxic environments.

bioRxiv preprint doi: https://doi.org/10.1101/2023.05.05.539519; this version posted May 5, 2023. The copyright holder for this preprint (which was not certified by peer review) is the author/funder, who has granted bioRxiv a license to display the preprint in perpetuity. It is made available under aCC-BY 4.0 International license.

As our molecular data suggest that ADR-1 binding to *pqm-1* mRNA in the absence of *adr-2* results in altered *pqm-1* expression, we sought to determine if loss of ADR-1 RNA binding could influence the survival of *adr-2(-)* animals to hypoxia. An independent set of hypoxia survival experiments were performed using wildtype, *pqm-1(-)* and *adr-2(-)* animals along with the *adr-2(-)*;ADR-1 dsRBD1 mutant animals. Consistent with the transgenic animals assayed in our study, compared to wildtype animals, both *pqm-1(-)* and *adr-2(-)* animals showed a significantly increased hypoxic survival (Figure 5B, Supplemental Figure S3). Compellingly, *adr-2(-)* animals lacking ADR-1 RNA binding function showed hypoxic survival similar to wildtype animals (Figure 5B). Together, these results suggest that neural PQM-1 is a key mediator of hypoxic survival and that binding of ADR-1 to *pqm-1* mRNA in the nervous system affects the animal's ability to survive hypoxic stress.

## Discussion

In these studies, we determined the tissue-specific contributions of ADAR proteins in regulating the insulin signaling pathway in *C. elegans*. Our data revealed unique ADR-1 RNA binding that occurs in the nervous system specifically in the absence of *adr-2*. As a previous study indicated heterodimer formation between ADR-1 and ADR-2 [46], studies have focused on understanding how ADR-1 facilitates ADR-2 binding to mRNAs to promote editing [27, 33, 46]. However, several other studies have also revealed that ADR-1 competes with ADR-2 for binding certain mRNAs, which can lead to decreased editing levels in transcripts [37, 50]. Together these studies suggest that the relationship between ADR-1 and ADR-2 is complex and may vary based on the tissue and developmental stage of the animals as well as on the individual transcript. In previous transcriptome-wide studies of ADR-1 mRNA binding, it was noted that ADR-1 binds nearly 1200 transcripts in wildtype worms and while ADR-1 is bound to nearly 80% of these in animals lacking *adr-2*, ADR-1 also uniquely bound nearly 400 mRNAs in the absence of *adr-2* [35]. The impact of ADR-1 binding to these unique targets has not been investigated. However, as our study identifies important biological consequences of ADR-1 binding to *pqm-1* specifically in the absence of *adr-2*, the impact of ADR-1 binding should be explored further. Additionally, as we observed that, upon feeding, *adr-2(-)* animals did not exhibit altered expression of genes downstream of the insulin signaling pathway (Figure 1C), it is possible that the presence of nutrients impacts ADR-1 binding to *pqm-1*. How environmental factors can influence ADAR target recognition is relatively unexplored and is an exciting future direction.

Our studies also revealed that loss of *adr-2* did not globally impact insulin signaling in neural cells, but instead, lead to further repression of genes negatively regulated in response to reduced insulin signaling (Supplemental Figure S2). Previous studies have indicated that the promoters of these genes contain an overrepresented sequence (CTTATCA), referred to as the DAE (DAF-16 associated element) [42] due to changes in expression of these genes upon loss of *daf-16* but lack of direct binding by DAF-16 [20]. The downregulation of over 150 DAE-containing genes in neural cells lacking *adr-2* suggested a global regulator of these genes was altered. Previous studies have identified the transcription factor PQM-1 as an important factor regulating DAE-containing genes in L4 animals [20]. Herein, we found that loss of *adr-2* resulted in a

bioRxiv preprint doi: https://doi.org/10.1101/2023.05.05.539519; this version posted May 5, 2023. The copyright holder for this preprint (which was not certified by peer review) is the author/funder, who has granted bioRxiv a license to display the preprint in perpetuity. It is made available under aCC-BY 4.0 International license.

neural-specific decrease in *pqm-1* expression, but decreased expression of the DAE-containing genes, *dod-17*, *dod-19* and *dod-24* in both neural cells and the intestine. Transcription from the *pqm-1* promoter was observed in the nervous system and the intestine in early studies surveying transcription factor expression in *C. elegans* [51]. More recent studies reported that PQM-1:GFP translational fusions exhibited strong intestinal expression, but neural expression was not observed [20, 52]. With these observations, it is not surprising that several recent studies have reported that PQM-1 has important impacts on intestinal gene expression [47, 53]. However, consequences of loss of *pqm-1* specifically in neural cells has also been previously reported for transgenic animals that have altered proteostasis networks, specifically transcellular chaperone signaling [52]. Here, we have added to that body of work by identifying molecular changes that occur in neural cells with reduced *pqm-1* expression.

Our studies also indicate that *pqm-1* expression solely within the nervous system is sufficient to promote expression of *dod-17*, *dod-19* and *dod-24* throughout the L1-arrested animal, providing the first evidence that PQM-1 can regulate gene expression in a cell non-autonomous manner. At present, it is unclear whether the cell non-autonomous regulation is dependent upon insulin signaling or if the downstream genes are affected by loss of *daf-2* [42] due to the impacts of DAF-2 on PQM-1 function in the nervous system. Our neural RNA-seq data did identify several insulin-like peptides (ILPs), including *ins-4*, *ins-5*, *ins-26*, *ins-35* and *daf-28* with significantly reduced expression in *adr-2(-)* neural cells (Supplemental Figure S4). Previous studies have shown that all of these ILPs are DAF-2 agonists [54-59]. Thus, it is possible that PQM-1 promotes expression of signaling molecules in the nervous system that relay information to the intestine to promote expression of the DAE-containing genes.

Another major unanswered question is what transcription factor could be mediating transcriptional control of the DAE-containing genes in the intestine. Previous studies of *C. elegans* transcription factors revealed an enrichment in DAE-containing sequences within the bound regions of 13 different proteins [20]. While PQM-1 was at the top of this list, it is possible that one of the other 12 transcription factors could be promoting transcription of DAE-containing genes in the intestine. Focusing on the promoters of *dod-17*, *dod-19* and *dod-24* specifically, chromatin immunoprecipitation (ChIP) sequencing studies have identified binding sites for three transcription factors, PQM-1, FOS-1 and NHR-28 [60], but only FOS-1 and PQM-1 are present at the promoters of all three genes. FOS-1 expression and function in somatic gonad cells and anchor cells is well established [61] and to date, there is no evidence that FOS-1 is expressed in intestinal cells. However, it is possible that in L1-arrested animals, FOS-1 expression changes and intestinal transcriptional activity could occur. In this same context, it is possible that other transcription factors occupy the *dod-17*, *dod-19* and *dod-24* promoters within intestinal tissue to promote transcription during L1-arrest. Future studies should screen for factors needed specifically in the intestine for proper expression of DAE-containing genes; however, this may prove challenging in L1-arrested animals, where standard RNA interference (RNAi) by feeding cannot be employed.

Our work establishes a novel role for PQM-1 in hypoxic survival of L1-arrested animals. While a majority of L1-arrested wildtype animals die from acute exposure to high ($\geq$10mM) doses of $CoCl_2$, *pqm-1(-)* animals exhibited significantly increased

bioRxiv preprint doi: https://doi.org/10.1101/2023.05.05.539519; this version posted May 5, 2023. The copyright holder for this preprint (which was not certified by peer review) is the author/funder, who has granted bioRxiv a license to display the preprint in perpetuity. It is made available under aCC-BY 4.0 International license.

survival. It was previously reported that loss of *pqm-1* resulted in increased survival of L4 animals placed either in a hypoxia chamber for 16 hours or exposed to low (5 mM) $CoCl_2$ for 20 hours [47]. Together these data indicate that PQM-1 is a negative regulator of hypoxic survival across developmental timescales. However, it is unclear whether the cellular role of PQM-1 is the same in larval and adult animals. Our phenotypic data revealed that PQM-1 function in neural cells is critical for its function as a negative regulator of hypoxic survival in L1-arrested animals. The previous study reported that PQM-1 promoted intestinal lipid levels and yolk protein transport to developing oocytes under oxygen depletion in adult animals [47]. However, it is important to note that direct binding of PQM-1 to the promoters of genes underlying the metabolic changes during adult hypoxic exposure was not demonstrated, thus it would be interesting to determine whether PQM-1 functions within the intestine or cell non-autonomously regulates hypoxic survival of adult animals.

At present, the physiological role for the negative regulation of survival by PQM-1 is unknown. Clearly on a cellular level, the ability to undergo metabolic changes that allow survival to hypoxia is a major aspect of oncogenesis; thus, players that keep this function in check are important. However, it is also well established in model organisms, including *C. elegans*, that adult animals reared under hypoxic conditions live longer than animals reared in normoxic conditions [62]. While promoting overall survival, the response to hypoxia is an energy intensive process that disrupts cellular proteostasis [63]; thus, to preserve energy and maintain equilibrium, it is likely equally important to control levels of hypoxic responses. Interestingly, a recent study revealed that fasted animals have an altered response to hypoxia and that the DAF-2 pathway, independent of DAF-16, plays an important role in this response [64]. It would be interesting to see if the role we identified for PQM-1 in L1 animals hatched in the absence of food is also involved in the coordinated response of adult animals to nutritional state and hypoxia. Furthermore, as exposure to limiting oxygen or nutrients has been reported to have transgenerational effects on descendants' metabolic programming, behavior and fecundity in *C. elegans* [65-67], exploring the role of PQM-1 in these processes may shed light on the physiological role of negative regulation of hypoxic survival.

## Materials and Methods

### *C. elegans strains and maintenance*

All worms were maintained under standard laboratory conditions on nematode growth media seeded with *Escherichia coli* OP50 [68]. The following previously generated strains were used in this study: Bristol strain N2, BB19 (*adr-1(tm668)*) [69], BB20 (*adr-2(ok735)*) [69], BB21 (*adr-1(tm668);adr-2(ok735)*) [69], HAH22 (*adr-2(gk777511)* [70] agIs6[*dod-24*::GFP] [43], *daf-2(m596)* [41], *pqm-1(ok485)* [45]. Neural cells were isolated from HAH45 (*prab3*::*rfp*::*C35E7.6* 3'UTR; *prab3*::*gfp*::*unc-54* 3' UTR; *unc-119* genomic rescue) and HAH46 (*adr-2(ok735)*; *prab3*::*rfp*::*C35E7.6* 3'UTR; *prab3*::*gfp*::*unc-54* 3' UTR; *unc-119* genomic rescue).

Strains generated in this study include HAH23 (BB20 + blmEx18(*Y75B8A.8* 3' UTR hairpin construct in *prab3::*GFP::*unc-54* 3' UTR (pHH340); *prab3*::3XFLAG ADR-2 cDNA::*unc-54 3'* UTR (pHH438)), HAH24 (BB20 + blmEx19(*Y75B8A.8 3' UTR* hairpin construct in *prab3*::GFP::*unc-54* 3' UTR Clone vector (pHH340)), HAH25 (BB19 +

bioRxiv preprint doi: https://doi.org/10.1101/2023.05.05.539519; this version posted May 5, 2023. The copyright holder for this preprint (which was not certified by peer review) is the author/funder, who has granted bioRxiv a license to display the preprint in perpetuity. It is made available under aCC-BY 4.0 International license.

blmEx20(*prab3::*GFP::*unc-54* 3' UTR (pHH21); *prab3::*3XFLAG ADR-1::*unc-54* 3' UTR (pHH512))), HAH26 (BB21+ blmEx20(*prab3::*GFP::*unc-54* 3' UTR(pHH21); *prab3::*3XFLAG ADR-1::*unc-54* 3' UTR (pHH512))), HAH27 (*adr-2(ok735)*, agIs6[*dod-24*::GFP]), HAH28 (BB20 + blmEx18(*Y75B8A.8* 3' UTR hairpin construct in *prab3::*GFP::*unc-54* 3' UTR (pHH340); *prab3*::3XFLAG ADR-2 cDNA::*unc-54 3'* UTR (pHH438), agIs6[*dod-24*::GFP]), HAH29 (*adr-2(ok735)*, *daf-2(m596)*), HAH30 (wildtype), HAH31 (*daf-2(m596)*), HAH32 (*adr-2(ok735)*), HAH33 (*adr-2(ok735)*, *daf-2(m596)*), HAH42 (HAH38+ blmEx19(*Y75B8A.8* 3' UTR hairpin construct in *prab3::*GFP::*unc-54* 3' UTR (pHH340))), HAH43 (HAH38+blmEx21(*Y75B8A.8* 3' UTR hairpin construct in *prab3::*GFP::*unc-54* 3' UTR (pHH340); *prab3*::*pqm-1*::*unc-54* 3' UTR (pHH549))), HAH47 (3X FLAG ADR-1 dsRBD1 (K223E, K224A, K227A) CRISPR).

Animals created by microinjection (HAH23-HAH26, HAH28, HAH40-HAH44) used standard microinjection techniques and were passaged by selecting worms that contained the GFP co-injection marker. The injection mix contained 20 ng/µl of the co-injection marker and 1 ng/µl of the transgene of interest.

Animals created by CRISPR modification (HAH47) used standard microinjection techniques and were identified as rolling F1 progeny and non-rolling F2 progeny. Injection mix for the ADR-1 dsRBD1 mutant strain included 1.5 µM Cas9 (IDT, Alt-R Cas9 nuclease V3), 4 µM tracrRNA (IDT), 4µM of crRNA (IDT)(HH3088) (Supplemental Table S2), 37 ng/µl *rol-6* plasmid (HAH293) and 4µM of repair template ssODN (HH3089) (Supplemental Table S2) containing the mutation in ADR-1 dsRBD1(KKxxK-EAxxA). Genomic modifications were verified using Sanger sequencing and ADR-1 expression was verified using western blot.

Crosses were performed by putting 9-10 males and 1 hermaphrodite on mating plates and genotyping was performed for the F1 progeny and F2 progeny using primers mentioned in Supplemental Table S2. The specific crosses performed included: creation of HAH27 by crossing agIs6[*dod-24*::GFP] hermaphrodites to BB20 males, creation of HAH28 by crossing HAH27 hermaphrodites to HAH23 males, creation of HAH29 by crossing *daf-2(m596)* hermaphrodites to BB20 males, creation of HAH34 by crossing *pqm-1(ok485)* hermaphrodites to N2 males, creation of HAH35 (wildtype), HAH37 (*adr-2(ok735)*), HAH38 (*pqm-1(ok485)*), HAH39 (*adr-2(ok735); pqm-1(ok485)*) by crossing HAH34 hermaphrodites to BB20 males, creation of HAH40 (BB20 + blmEx19(*Y75B8A.8* 3' UTR hairpin construct in *prab3::*GFP::*unc-54* 3' UTR (pHH340))) and HAH41 (blmEx19(*Y75B8A.8* 3' UTR hairpin construct in *prab3*::GFP::*unc-54* 3' UTR (pHH340))) by crossing HAH24 hermaphrodites to N2 males, creation of HAH44 (BB20+ blmEx21(*Y75B8A.8* 3' UTR hairpin construct in *prab3::*GFP::*unc-54* 3' UTR (pHH340); *prab3*::*pqm-1*::*unc-54* 3' UTR (pHH549))) by crossing HAH43 hermaphrodites to BB20 males, creation of HAH48 (wildtype), HAH49 (*adr-2(ok735)*) and HAH50 (ADR-1 dsRBD1 (KKxxK-EAxxA) CRISPR) by crossing HAH47 hermaphrodites to BB20 males

***Cloning***

To generate the neural ADR-2 complementary DNA (cDNA) expressing animals, the *adr-2* cDNA sequence was amplified from a plasmid with primers HH1962 and HH1963 (Supplemental Table S2). This fragment was cut with restriction enzymes BglII and SalI and then cloned into plasmid pHH326 (*prab3::*GFP::*unc-54* 3' UTR) to generate a

bioRxiv preprint doi: https://doi.org/10.1101/2023.05.05.539519; this version posted May 5, 2023. The copyright holder for this preprint (which was not certified by peer review) is the author/funder, who has granted bioRxiv a license to display the preprint in perpetuity. It is made available under aCC-BY 4.0 International license.

plasmid expressing neural *adr-2* cDNA. The sequence of the *adr-2* region cloned into the plasmid was confirmed using Sanger sequencing.

To generate the neural ADR-1 expressing animals, the *rab3* promoter sequence was amplified from plasmid pHH326 (*prab3::*GFP::*unc-54* 3' UTR) with primers HH170 and HH2771 (Supplemental Table S2). This fragment was cloned into plasmid pHH99 (pBluescript 3X FLAG genomic *adr-1*) previously published [33], with restriction enzymes KpnI and PstI to generate plasmid pHH512 with *prab3:*:3XFLAG ADR-1. The sequence of the *rab3* promoter cloned into the plasmid was confirmed using Sanger sequencing.

The vector used to express *pqm-1* in the nervous system, pWorm[Exp]-rab-3>cel_pqm-1, was constructed by VectorBuilder. The vector ID is VB221230-1025zug, which can be used to retrieve detailed vector information from vectorbuilder.com.

***Gene set enrichment analysis***

Gene set enrichment analysis was performed using the online WormCat software [38] for upregulated and downregulated genes identified from comparing the wildtype and *adr-2(-)* neural RNA-seq datasets.

***Bleaching***

Synchronized first larval stage (L1) animals were obtained by bleaching with 5M NaOH and Clorox solution. After bleach solution was added, animals were incubated on a shaker at 20°C for 7 minutes and then spun down to collect embryos. Collected embryos were washed with 1X M9 buffer (22.0 mM $KH_2PO_4$, 42.3 mM $Na_2HPO_4$, 85.6 mM NaCl, 1 mM $MgSO_4$) solution thrice. The animals were incubated overnight in 1X M9 solution at 20°C. Next day, hatched L1 worms were spun down and washed again with 1X M9 solution thrice.

***Neural cell isolation and COPAS sorting***

Neural cells were isolated from synchronized first larval stage worms as previously described [27] and filtered into sterile FACS tubes. Briefly, staining with near IR live/dead fixable dye (Invitrogen) of the isolated neural cells was done before performing FACS sorting. The BD FACSAria II sorter was used to separate the GFP+ neural cells from the non-GFP cells, and FACSDiva 6.1.1 software was used to analyze the sort (IU Flow Cytometry Core Facility). Sorted neural cells were collected into conical tubes with TRIzol (Invitrogen), snap-frozen in liquid nitrogen and stored at −80°C. For sorting transgenic animals, the COPAS BioSelect instrument (IU Flow Cytometry Core Facilty) was used to isolate GFP+ animals based on Time of Flight (TOF) and Extinction (Ext). 250 transgenic GFP+ animals were sorted per strain and collected on unseeded 10 cm NGM plates.

***Bioinformatics analysis for differential gene expression***

N2 and *adr-2(-)* L1 neural datasets generated in [37] under accession number GSE1151916 were downloaded and analyzed. 75 bp single-end stranded RNA-sequencing reads were subjected to adaptor trimming and aligned to the *C. elegans* genome (WS275) using STAR (v2.7.8a) with the parameters: [*runThreadN 8*, *outFilterMultimapNmax 1*, *outFilterScoreMinOverLread 0.66*, *outFilterMismatchNmax 10*, *outFilterMismatchNoverLmax: 0.3*]. Indexing of the aligned bam files was performed

bioRxiv preprint doi: https://doi.org/10.1101/2023.05.05.539519; this version posted May 5, 2023. The copyright holder for this preprint (which was not certified by peer review) is the author/funder, who has granted bioRxiv a license to display the preprint in perpetuity. It is made available under aCC-BY 4.0 International license.

using samtools (v1.3.1) and featureCounts (v2.0.1) was used to generate the raw read counts file. DESeq2 library (v1.26.0) on R studio [71] was used to process the raw read counts and generate the counts.csv file used for differential gene expression analysis.

***RNA isolation and quantitative real-time PCR (qPCR)***

RNA extraction was performed using TRIzol (Invitrogen) reagent and DNA contamination was removed by treatment with TURBO DNase (Ambion) followed by the RNeasy Extraction kit (Qiagen) and stored at − 80°C. Concentrations of the RNA samples and presence of any contamination with organic and protein components was determined using a Nanodrop (Fisher Scientific). For qPCR experiments using RNA from L1 animals, 2 ug of DNase-treated RNA was reverse transcribed into cDNA using Superscript III (Invitrogen) with random hexamers (Fisher Scientific) and oligo dT (Fisher Scientific) primers. For qPCR experiments using RNA from neural cells or COPAS sorted transgenic animals, the whole 12 ul was reverse transcribed into cDNA. Following reverse transcription of RNA from L1 animals, 20 µL of water was added to the cDNA. For RNA immunoprecipitation experiments, 200 ng RNA for inputs and the whole 12 ul of IP samples was reverse transcribed into cDNA and no water was added to the cDNA. Gene expression was determined using SybrFast Master Mix water and gene-specific primers (Supplemental Table S2) on a Thermofisher Quantstudio 3 instrument. The primers designed for qPCR (Supplemental Table S2) spanned an exon-exon junction to prevent detection of genomic DNA in the samples. Melting curves were generated for all primer pairs used to ensure high quality of qPCR products. For each gene analyzed, a standard curve of eight to ten samples of ten-fold serial dilutions of the amplified product were used to generate a standard curve of cycle threshold versus the relative concentration of amplified product. Standard curves were plotted on a logarithmic scale in relation to concentration and fit with a linear line. Fit ($r^2$) values were around 0.99 and at least 7 data points fell within the standard curve. Each cDNA measurement was performed in three technical replicates, and each experiment was performed in three biological replicates.

***Fluorescence microscopy***

Synchronized L1 animals were anesthetized on agarose pads containing sodium azide followed by a coverslip. Images were taken using the Leica SP8 Scanning Confocal Microscope (IU Light Microscopy Imaging Core) and the 10x objective. Each image was taken with the intestinal cells and head ganglia region in focus. For each trial, exposure time was calibrated to minimize the number of saturated pixels for that set of animals. ImageJ bundled with Java 8 software was used to quantify the total intensity of fluorescence per worm as measured by intensity of each pixel in the selected area of a frame (i.e. the worm).

***RNA immunoprecipitation***

Synchronized L1 worms were washed with IP buffer (50 mM HEPES [pH 7.4], 70 mM K-Acetate, 5 mM Mg-Acetate, 0.05% NP-40 and 10% glycerol) containing a mini EDTA-free cOmplete protease inhibitor tablet (Roche) and UV crosslinked (3 J/cm2) using the Spectrolinker (Spectronics). The worms were then frozen into pellets using liquid nitrogen and stored at -80°C. The frozen worm pellets were ground on dry ice with a

bioRxiv preprint doi: https://doi.org/10.1101/2023.05.05.539519; this version posted May 5, 2023. The copyright holder for this preprint (which was not certified by peer review) is the author/funder, who has granted bioRxiv a license to display the preprint in perpetuity. It is made available under aCC-BY 4.0 International license.

cold mortar and pestle, and the cell lysate was centrifuged at maximum speed for 10 minutes to remove cellular debris. Protein concentration was measured using Bradford reagent (Sigma) and the entire L1 lysates were added to 25 ul magnetic Protein-G beads (Invitrogen) for preclearing. After incubation for 1 hour on a rotator at 4°C, 500 ug of the L1 lysate from the supernatant was added to 25 ul anti-FLAG magnetic beads (Sigma). After incubation for 1 hour on a rotator at 4°C, protein-bound beads were washed with wash buffer thrice (0.5 M NaCl, 160 mM Tris-HCl [pH 7.5], 0.1% NP-40, 0.25% Triton X-100) containing a mini EDTA-free cOmplete protease inhibitor tablet (Roche). A portion of the IP (2/5) was stored in 2X SDS loading buffer and used for immunoblotting. The remaining beads were incubated with 1 ul RNasin (Fisher) and 0.5 µl of 20 mg/ml Proteinase K (NEB) at 42°C and 1200 rpm for 15 minutes in a thermomixer. RNA was isolated and qPCR was performed as described above.

### *Immunoblotting*

Protein lysates were prepared as mentioned above. Protein lysates were boiled for five minutes and 100 ug of IP lysates and 10 ug of input lysates were subjected to SDS-PAGE. The same immunoblot was treated with antibodies against FLAG (Sigma, M8823) and β-Actin (Cell Signaling, 8457S) after cutting the blot. Protein bands were visualized using enhanced chemiluminescent detection SuperSignal West Femto Maximum Sensitivity Substrate (Fisher). The immunoblot images without saturation were acquired using Image Lab software (version 6.1.0 build 7) in the BIO-RAD ChemiDoc MP imaging system.

### *Cobalt chloride exposure assays*

These assays were performed as previously described [49] with slight modifications. Briefly, cobalt(II) chloride hexahydrate ($CoCl_2$) powder (Sigma-Aldrich) was used to make a 0.1 M stock solution with distilled water and then working stocks of varying concentrations were prepared in 85 mM NaCl. Bleaching according to above mentioned conditions was performed to obtain L1-arrested animals. After washing the hatched animals twice with 85 mM NaCl, 5000 L1 animals per strain were exposed to $CoCl_2$ of varying concentrations in a total volume of 500 ul for two hours. After exposure, the worms were washed twice with 85 mM NaCl to remove any residual $CoCl_2$ and other debris. After washing, 40 worms per strain were transferred to 35 mm NGM plates seeded with OP50 and incubated at 20°C for twenty-four hours. After the incubation, alive and dead worms were counted in triplicates for each strain and three biological replicates for both the transgenic and non-transgenic sets of worms. Genotypes were blinded before the bleaching to reduce bias.

**Acknowledgements**

We thank Christiane Hassel (IUB- Flow Cytometry Core Facility) for assisting in COPAS sorting of transgenic animals. We thank Dr. Andras Kun (IUB- Light Microscopy Imaging Center) for the training and facilitating usage of the confocal microscope. We thank current members of the Hundley lab, Dr. Chinnu Salim, Boyoon Yang, Emily Erdmann, and Mary Skelly for careful reading of the manuscript. We thank graduate student Shefali Shefali for her tremendous help in taking the confocal images and Boyoon Yang for assisting in the masking of genotypes for the survival assays.

bioRxiv preprint doi: https://doi.org/10.1101/2023.05.05.539519; this version posted May 5, 2023. The copyright holder for this preprint (which was not certified by peer review) is the author/funder, who has granted bioRxiv a license to display the preprint in perpetuity. It is made available under aCC-BY 4.0 International license.

**Financial Disclosure**

This work was supported by the National Science Foundation (Award 191750 to HAH), National Institute of Health (R01 GM130759 to HAH) and the John R. and Wendy L. Kindig Fellowship (to AM). Some strains were provided by the CGC, which is funded by NIH Office of Research Infrastructure Programs (P40 OD010440). The funders had no role in study design, data collection and analysis, decision to publish, or preparation of the manuscript.

**Author Contributions**

Designed the experiments: A.M, H.A.H.
Created reagents: A.D., P.V., A.M., H.A.H.
Performed the experiments: A.N., A.M.
Performed the bioinformatics analysis: A.M.
Wrote and edited the manuscript: A.M., H.A.H.

**References**

1. Rashid S, Wong C, Roy R. Developmental plasticity and the response to nutrient stress in Caenorhabditis elegans. Dev Biol. 2021;475:265-76. Epub 2021/02/08. doi: 10.1016/j.ydbio.2021.01.015. PubMed PMID: 33549550.
2. Padilla PA, Nystul TG, Zager RA, Johnson AC, Roth MB. Dephosphorylation of cell cycle-regulated proteins correlates with anoxia-induced suspended animation in Caenorhabditis elegans. Mol Biol Cell. 2002;13(5):1473-83. doi: 10.1091/mbc.01-12-0594. PubMed PMID: 12006646; PubMed Central PMCID: PMCPMC111120.
3. Baugh LR. To grow or not to grow: nutritional control of development during Caenorhabditis elegans L1 arrest. Genetics. 2013;194(3):539-55. Epub 2013/07/05. doi: 10.1534/genetics.113.150847. PubMed PMID: 23824969; PubMed Central PMCID: PMCPMC3697962.
4. Mata-Cabana A, Perez-Nieto C, Olmedo M. Nutritional control of postembryonic development progression and arrest in Caenorhabditis elegans. Adv Genet. 2021;107:33-87. Epub 2021/03/02. doi: 10.1016/bs.adgen.2020.11.002. PubMed PMID: 33641748.
5. Allen E, Ren J, Zhang Y, Alcedo J. Sensory systems: their impact on C. elegans survival. Neuroscience. 2015;296:15-25. Epub 2014/07/06. doi: 10.1016/j.neuroscience.2014.06.054. PubMed PMID: 24997267; PubMed Central PMCID: PMCPMC4282626.
6. Das S, Ooi FK, Cruz Corchado J, Fuller LC, Weiner JA, Prahlad V. Serotonin signaling by maternal neurons upon stress ensures progeny survival. Elife. 2020;9. Epub 2020/04/24. doi: 10.7554/eLife.55246. PubMed PMID: 32324136; PubMed Central PMCID: PMCPMC7237211.
7. Handley A, Wu Q, Sherry T, Cornell R, Pocock R. Diet-responsive transcriptional regulation of insulin in a single neuron controls systemic metabolism. PLoS Biol. 2022;20(5):e3001655. Epub 2022/05/21. doi: 10.1371/journal.pbio.3001655. PubMed PMID: 35594303; PubMed Central PMCID: PMCPMC9162364.

bioRxiv preprint doi: https://doi.org/10.1101/2023.05.05.539519; this version posted May 5, 2023. The copyright holder for this preprint (which was not certified by peer review) is the author/funder, who has granted bioRxiv a license to display the preprint in perpetuity. It is made available under aCC-BY 4.0 International license.

8. McLachlan IG, Kramer TS, Dua M, DiLoreto EM, Gomes MA, Dag U, et al. Diverse states and stimuli tune olfactory receptor expression levels to modulate food-seeking behavior. Elife. 2022;11. Epub 2022/09/01. doi: 10.7554/eLife.79557. PubMed PMID: 36044259; PubMed Central PMCID: PMCPMC9433090.
9. Makdissi S, Parsons BD, Di Cara F. Towards early detection of neurodegenerative diseases: A gut feeling. Front Cell Dev Biol. 2023;11:1087091. Epub 20230207. doi: 10.3389/fcell.2023.1087091. PubMed PMID: 36824371; PubMed Central PMCID: PMCPMC9941184.
10. Slominski RM, Raman C, Chen JY, Slominski AT. How cancer hijacks the body's homeostasis through the neuroendocrine system. Trends Neurosci. 2023;46(4):263-75. Epub 20230217. doi: 10.1016/j.tins.2023.01.003. PubMed PMID: 36803800; PubMed Central PMCID: PMCPMC10038913.
11. Miller HA, Dean ES, Pletcher SD, Leiser SF. Cell non-autonomous regulation of health and longevity. Elife. 2020;9. Epub 20201210. doi: 10.7554/eLife.62659. PubMed PMID: 33300870; PubMed Central PMCID: PMCPMC7728442.
12. Hodge F, Bajuszova V, van Oosten-Hawle P. The Intestine as a Lifespan- and Proteostasis-Promoting Signaling Tissue. Front Aging. 2022;3:897741. Epub 2022/07/14. doi: 10.3389/fragi.2022.897741. PubMed PMID: 35821863; PubMed Central PMCID: PMCPMC9261303.
13. Gonzalez A, Hall MN, Lin SC, Hardie DG. AMPK and TOR: The Yin and Yang of Cellular Nutrient Sensing and Growth Control. Cell Metab. 2020;31(3):472-92. Epub 2020/03/05. doi: 10.1016/j.cmet.2020.01.015. PubMed PMID: 32130880.
14. Majmundar AJ, Wong WJ, Simon MC. Hypoxia-inducible factors and the response to hypoxic stress. Mol Cell. 2010;40(2):294-309. Epub 2010/10/23. doi: 10.1016/j.molcel.2010.09.022. PubMed PMID: 20965423; PubMed Central PMCID: PMCPMC3143508.
15. Jia K, Chen D, Riddle DL. The TOR pathway interacts with the insulin signaling pathway to regulate C. elegans larval development, metabolism and life span. Development. 2004;131(16):3897-906. Epub 2004/07/16. doi: 10.1242/dev.01255. PubMed PMID: 15253933.
16. Szkudelski T, Szkudelska K. The relevance of AMP-activated protein kinase in insulin-secreting beta cells: a potential target for improving beta cell function? J Physiol Biochem. 2019;75(4):423-32. Epub 2019/11/07. doi: 10.1007/s13105-019-00706-3. PubMed PMID: 31691163; PubMed Central PMCID: PMCPMC6920233.
17. Kimura KD, Tissenbaum HA, Liu Y, Ruvkun G. daf-2, an insulin receptor-like gene that regulates longevity and diapause in Caenorhabditis elegans. Science. 1997;277(5328):942-6. Epub 1997/08/15. doi: 10.1126/science.277.5328.942. PubMed PMID: 9252323.
18. Zheng S, Chiu H, Boudreau J, Papanicolaou T, Bendena W, Chin-Sang I. A functional study of all 40 Caenorhabditis elegans insulin-like peptides. J Biol Chem. 2018;293(43):16912-22. Epub 2018/09/13. doi: 10.1074/jbc.RA118.004542. PubMed PMID: 30206121; PubMed Central PMCID: PMCPMC6204898.
19. Murphy CT, Hu PJ. Insulin/insulin-like growth factor signaling in C. elegans. WormBook. 2013:1-43. Epub 2014/01/08. doi: 10.1895/wormbook.1.164.1. PubMed PMID: 24395814; PubMed Central PMCID: PMCPMC4780952.

bioRxiv preprint doi: https://doi.org/10.1101/2023.05.05.539519; this version posted May 5, 2023. The copyright holder for this preprint (which was not certified by peer review) is the author/funder, who has granted bioRxiv a license to display the preprint in perpetuity. It is made available under aCC-BY 4.0 International license.

20. Tepper RG, Ashraf J, Kaletsky R, Kleemann G, Murphy CT, Bussemaker HJ. PQM-1 complements DAF-16 as a key transcriptional regulator of DAF-2-mediated development and longevity. Cell. 2013;154(3):676-90. Epub 2013/08/06. doi: 10.1016/j.cell.2013.07.006. PubMed PMID: 23911329; PubMed Central PMCID: PMCPMC3763726.
21. Biglou SG, Bendena WG, Chin-Sang I. An overview of the insulin signaling pathway in model organisms Drosophila melanogaster and Caenorhabditis elegans. Peptides. 2021;145:170640. Epub 2021/08/28. doi: 10.1016/j.peptides.2021.170640. PubMed PMID: 34450203.
22. Lee H, Lee SV. Recent Progress in Regulation of Aging by Insulin/IGF-1 Signaling in Caenorhabditis elegans. Mol Cells. 2022;45(11):763-70. Epub 2022/11/17. doi: 10.14348/molcells.2022.0097. PubMed PMID: 36380728; PubMed Central PMCID: PMCPMC9676989.
23. Porte D, Jr., Baskin DG, Schwartz MW. Insulin signaling in the central nervous system: a critical role in metabolic homeostasis and disease from C. elegans to humans. Diabetes. 2005;54(5):1264-76. Epub 2005/04/28. doi: 10.2337/diabetes.54.5.1264. PubMed PMID: 15855309.
24. Kenyon C, Chang J, Gensch E, Rudner A, Tabtiang R. A C. elegans mutant that lives twice as long as wild type. Nature. 1993;366(6454):461-4. Epub 1993/12/02. doi: 10.1038/366461a0. PubMed PMID: 8247153.
25. Wolkow CA, Kimura KD, Lee MS, Ruvkun G. Regulation of C. elegans life-span by insulinlike signaling in the nervous system. Science. 2000;290(5489):147-50. Epub 2000/10/06. doi: 10.1126/science.290.5489.147. PubMed PMID: 11021802.
26. Martinez BA, Reis Rodrigues P, Nunez Medina RM, Mondal P, Harrison NJ, Lone MA, et al. An alternatively spliced, non-signaling insulin receptor modulates insulin sensitivity via insulin peptide sequestration in C. elegans. Elife. 2020;9. Epub 2020/02/26. doi: 10.7554/eLife.49917. PubMed PMID: 32096469; PubMed Central PMCID: PMCPMC7041946.
27. Deffit SN, Yee BA, Manning AC, Rajendren S, Vadlamani P, Wheeler EC, et al. The C. elegans neural editome reveals an ADAR target mRNA required for proper chemotaxis. Elife. 2017;6. Epub 2017/09/20. doi: 10.7554/eLife.28625. PubMed PMID: 28925356; PubMed Central PMCID: PMCPMC5644944.
28. Licht K, Jantsch MF. Rapid and dynamic transcriptome regulation by RNA editing and RNA modifications. J Cell Biol. 2016;213(1):15-22. Epub 2016/04/06. doi: 10.1083/jcb.201511041. PubMed PMID: 27044895; PubMed Central PMCID: PMCPMC4828693.
29. Rosenthal JJ. The emerging role of RNA editing in plasticity. J Exp Biol. 2015;218(Pt 12):1812-21. Epub 2015/06/19. doi: 10.1242/jeb.119065. PubMed PMID: 26085659; PubMed Central PMCID: PMCPMC4487009.
30. Eisenberg E, Levanon EY. A-to-I RNA editing - immune protector and transcriptome diversifier. Nat Rev Genet. 2018;19(8):473-90. Epub 2018/04/26. doi: 10.1038/s41576-018-0006-1. PubMed PMID: 29692414.
31. Arribere JA, Kuroyanagi H, Hundley HA. mRNA Editing, Processing and Quality Control in Caenorhabditis elegans. Genetics. 2020;215(3):531-68. Epub 2020/07/08. doi: 10.1534/genetics.119.301807. PubMed PMID: 32632025; PubMed Central PMCID: PMCPMC7337075.

bioRxiv preprint doi: https://doi.org/10.1101/2023.05.05.539519; this version posted May 5, 2023. The copyright holder for this preprint (which was not certified by peer review) is the author/funder, who has granted bioRxiv a license to display the preprint in perpetuity. It is made available under aCC-BY 4.0 International license.

32. Tonkin LA, Saccomanno L, Morse DP, Brodigan T, Krause M, Bass BL. RNA editing by ADARs is important for normal behavior in Caenorhabditis elegans. EMBO J. 2002;21(22):6025-35. Epub 2002/11/12. doi: 10.1093/emboj/cdf607. PubMed PMID: 12426375; PubMed Central PMCID: PMCPMC137199.
33. Washburn MC, Kakaradov B, Sundararaman B, Wheeler E, Hoon S, Yeo GW, et al. The dsRBP and inactive editor ADR-1 utilizes dsRNA binding to regulate A-to-I RNA editing across the C. elegans transcriptome. Cell Rep. 2014;6(4):599-607. doi: 10.1016/j.celrep.2014.01.011. PubMed PMID: 24508457; PubMed Central PMCID: PMCPMC3959997.
34. Erdmann EA, Mahapatra A, Mukherjee P, Yang B, Hundley HA. To protect and modify double-stranded RNA - the critical roles of ADARs in development, immunity and oncogenesis. Crit Rev Biochem Mol Biol. 2021;56(1):54-87. Epub 2020/12/29. doi: 10.1080/10409238.2020.1856768. PubMed PMID: 33356612; PubMed Central PMCID: PMCPMC8019592.
35. Ganem NS, Ben-Asher N, Manning AC, Deffit SN, Washburn MC, Wheeler EC, et al. Disruption in A-to-I Editing Levels Affects C. elegans Development More Than a Complete Lack of Editing. Cell Rep. 2019;27(4):1244-53 e4. Epub 2019/04/25. doi: 10.1016/j.celrep.2019.03.095. PubMed PMID: 31018137.
36. Szymczak F, Cohen-Fultheim R, Thomaidou S, de Brachene AC, Castela A, Colli M, et al. ADAR1-dependent editing regulates human beta cell transcriptome diversity during inflammation. Front Endocrinol (Lausanne). 2022;13:1058345. Epub 2022/12/16. doi: 10.3389/fendo.2022.1058345. PubMed PMID: 36518246; PubMed Central PMCID: PMCPMC9742459.
37. Rajendren S, Dhakal A, Vadlamani P, Townsend J, Deffit SN, Hundley HA. Profiling neural editomes reveals a molecular mechanism to regulate RNA editing during development. Genome Res. 2021;31(1):27-39. Epub 20201218. doi: 10.1101/gr.267575.120. PubMed PMID: 33355311; PubMed Central PMCID: PMCPMC7849389.
38. Holdorf AD, Higgins DP, Hart AC, Boag PR, Pazour GJ, Walhout AJM, et al. WormCat: An Online Tool for Annotation and Visualization of Caenorhabditis elegans Genome-Scale Data. Genetics. 2020;214(2):279-94. Epub 2019/12/08. doi: 10.1534/genetics.119.302919. PubMed PMID: 31810987; PubMed Central PMCID: PMCPMC7017019.
39. Fung C, Vanden Berghe P. Functional circuits and signal processing in the enteric nervous system. Cell Mol Life Sci. 2020;77(22):4505-22. Epub 2020/05/20. doi: 10.1007/s00018-020-03543-6. PubMed PMID: 32424438; PubMed Central PMCID: PMCPMC7599184.
40. Baugh LR, Hu PJ. Starvation Responses Throughout the Caenorhabditiselegans Life Cycle. Genetics. 2020;216(4):837-78. Epub 2020/12/04. doi: 10.1534/genetics.120.303565. PubMed PMID: 33268389; PubMed Central PMCID: PMCPMC7768255.
41. Hung WL, Hwang C, Gao S, Liao EH, Chitturi J, Wang Y, et al. Attenuation of insulin signalling contributes to FSN-1-mediated regulation of synapse development. EMBO J. 2013;32(12):1745-60. Epub 2013/05/15. doi: 10.1038/emboj.2013.91. PubMed PMID: 23665919; PubMed Central PMCID: PMCPMC3680742.
42. Murphy CT, McCarroll SA, Bargmann CI, Fraser A, Kamath RS, Ahringer J, et al. Genes that act downstream of DAF-16 to influence the lifespan of Caenorhabditis elegans.

bioRxiv preprint doi: https://doi.org/10.1101/2023.05.05.539519; this version posted May 5, 2023. The copyright holder for this preprint (which was not certified by peer review) is the author/funder, who has granted bioRxiv a license to display the preprint in perpetuity. It is made available under aCC-BY 4.0 International license.

Nature. 2003;424(6946):277-83. Epub 2003/07/08. doi: 10.1038/nature01789. PubMed PMID: 12845331.

43. Yamawaki TM, Berman JR, Suchanek-Kavipurapu M, McCormick M, Gaglia MM, Lee SJ, et al. The somatic reproductive tissues of C. elegans promote longevity through steroid hormone signaling. PLoS Biol. 2010;8(8). Epub 2010/09/09. doi: 10.1371/journal.pbio.1000468. PubMed PMID: 20824162; PubMed Central PMCID: PMCPMC2930862.
44. Zhang P, Judy M, Lee SJ, Kenyon C. Direct and indirect gene regulation by a life-extending FOXO protein in C. elegans: roles for GATA factors and lipid gene regulators. Cell Metab. 2013;17(1):85-100. Epub 2013/01/15. doi: 10.1016/j.cmet.2012.12.013. PubMed PMID: 23312285; PubMed Central PMCID: PMCPMC3969420.
45. Consortium CeDM. large-scale screening for targeted knockouts in the Caenorhabditis elegans genome. G3 (Bethesda). 2012;2(11):1415-25. Epub 2012/11/23. doi: 10.1534/g3.112.003830. PubMed PMID: 23173093; PubMed Central PMCID: PMCPMC3484672.
46. Rajendren S, Manning AC, Al-Awadi H, Yamada K, Takagi Y, Hundley HA. A protein-protein interaction underlies the molecular basis for substrate recognition by an adenosine-to-inosine RNA-editing enzyme. Nucleic Acids Res. 2018;46(18):9647-59. Epub 2018/09/12. doi: 10.1093/nar/gky800. PubMed PMID: 30202880; PubMed Central PMCID: PMCPMC6182170.
47. Heimbucher T, Hog J, Gupta P, Murphy CT. Author Correction: PQM-1 controls hypoxic survival via regulation of lipid metabolism. Nat Commun. 2020;11(1):6018. Epub 2020/11/22. doi: 10.1038/s41467-020-19868-6. PubMed PMID: 33219230; PubMed Central PMCID: PMCPMC7680132.
48. Padmanabha D, Padilla PA, You YJ, Baker KD. A HIF-independent mediator of transcriptional responses to oxygen deprivation in Caenorhabditis elegans. Genetics. 2015;199(3):739-48. Epub 2015/01/02. doi: 10.1534/genetics.114.173989. PubMed PMID: 25552276; PubMed Central PMCID: PMCPMC4349068.
49. Zheng F, Chen P, Li H, Aschner M. Drp-1-Dependent Mitochondrial Fragmentation Contributes to Cobalt Chloride-Induced Toxicity in Caenorhabditis elegans. Toxicol Sci. 2020;177(1):158-67. Epub 2020/07/04. doi: 10.1093/toxsci/kfaa105. PubMed PMID: 32617571; PubMed Central PMCID: PMCPMC7553700.
50. Washburn MC, Hundley HA. Trans and cis factors affecting A-to-I RNA editing efficiency of a noncoding editing target in C. elegans. RNA. 2016;22(5):722-8. Epub 2016/02/27. doi: 10.1261/rna.055079.115. PubMed PMID: 26917557; PubMed Central PMCID: PMCPMC4836646.
51. Reece-Hoyes JS, Shingles J, Dupuy D, Grove CA, Walhout AJ, Vidal M, et al. Insight into transcription factor gene duplication from Caenorhabditis elegans Promoterome-driven expression patterns. BMC Genomics. 2007;8:27. Epub 2007/01/25. doi: 10.1186/1471-2164-8-27. PubMed PMID: 17244357; PubMed Central PMCID: PMCPMC1785375.
52. O'Brien D, Jones LM, Good S, Miles J, Vijayabaskar MS, Aston R, et al. A PQM-1-Mediated Response Triggers Transcellular Chaperone Signaling and Regulates Organismal Proteostasis. Cell Rep. 2018;23(13):3905-19. Epub 2018/06/28. doi: 10.1016/j.celrep.2018.05.093. PubMed PMID: 29949773; PubMed Central PMCID: PMCPMC6045774.

bioRxiv preprint doi: https://doi.org/10.1101/2023.05.05.539519; this version posted May 5, 2023. The copyright holder for this preprint (which was not certified by peer review) is the author/funder, who has granted bioRxiv a license to display the preprint in perpetuity. It is made available under aCC-BY 4.0 International license.

53. Dowen RH, Breen PC, Tullius T, Conery AL, Ruvkun G. A microRNA program in the C. elegans hypodermis couples to intestinal mTORC2/PQM-1 signaling to modulate fat transport. Genes Dev. 2016;30(13):1515-28. Epub 2016/07/13. doi: 10.1101/gad.283895.116. PubMed PMID: 27401555; PubMed Central PMCID: PMCPMC4949325.
54. Chen Y, Baugh LR. Ins-4 and daf-28 function redundantly to regulate C. elegans L1 arrest. Dev Biol. 2014;394(2):314-26. Epub 2014/08/17. doi: 10.1016/j.ydbio.2014.08.002. PubMed PMID: 25128585.
55. Cornils A, Gloeck M, Chen Z, Zhang Y, Alcedo J. Specific insulin-like peptides encode sensory information to regulate distinct developmental processes. Development. 2011;138(6):1183-93. Epub 2011/02/24. doi: 10.1242/dev.060905. PubMed PMID: 21343369; PubMed Central PMCID: PMCPMC3042873.
56. Fernandes de Abreu DA, Caballero A, Fardel P, Stroustrup N, Chen Z, Lee K, et al. An insulin-to-insulin regulatory network orchestrates phenotypic specificity in development and physiology. PLoS Genet. 2014;10(3):e1004225. Epub 2014/03/29. doi: 10.1371/journal.pgen.1004225. PubMed PMID: 24675767; PubMed Central PMCID: PMCPMC3967928.
57. Hung WL, Wang Y, Chitturi J, Zhen M. A Caenorhabditis elegans developmental decision requires insulin signaling-mediated neuron-intestine communication. Development. 2014;141(8):1767-79. Epub 2014/03/29. doi: 10.1242/dev.103846. PubMed PMID: 24671950; PubMed Central PMCID: PMCPMC3978837.
58. Li W, Kennedy SG, Ruvkun G. daf-28 encodes a C. elegans insulin superfamily member that is regulated by environmental cues and acts in the DAF-2 signaling pathway. Genes Dev. 2003;17(7):844-58. Epub 2003/03/26. doi: 10.1101/gad.1066503. PubMed PMID: 12654727; PubMed Central PMCID: PMCPMC196030.
59. Patel DS, Fang LL, Svy DK, Ruvkun G, Li W. Genetic identification of HSD-1, a conserved steroidogenic enzyme that directs larval development in Caenorhabditis elegans. Development. 2008;135(13):2239-49. Epub 2008/05/23. doi: 10.1242/dev.016972. PubMed PMID: 18495818.
60. Boyle AP, Araya CL, Brdlik C, Cayting P, Cheng C, Cheng Y, et al. Comparative analysis of regulatory information and circuits across distant species. Nature. 2014;512(7515):453-6. Epub 2014/08/29. doi: 10.1038/nature13668. PubMed PMID: 25164757; PubMed Central PMCID: PMCPMC4336544.
61. Hiatt SM, Duren HM, Shyu YJ, Ellis RE, Hisamoto N, Matsumoto K, et al. Caenorhabditis elegans FOS-1 and JUN-1 regulate plc-1 expression in the spermatheca to control ovulation. Mol Biol Cell. 2009;20(17):3888-95. Epub 2009/07/03. doi: 10.1091/mbc.e08-08-0833. PubMed PMID: 19570917; PubMed Central PMCID: PMCPMC2735487.
62. Leiser SF, Fletcher M, Begun A, Kaeberlein M. Life-span extension from hypoxia in Caenorhabditis elegans requires both HIF-1 and DAF-16 and is antagonized by SKN-1. J Gerontol A Biol Sci Med Sci. 2013;68(10):1135-44. Epub 2013/02/20. doi: 10.1093/gerona/glt016. PubMed PMID: 23419779; PubMed Central PMCID: PMCPMC3779632.
63. Fawcett EM, Hoyt JM, Johnson JK, Miller DL. Hypoxia disrupts proteostasis in Caenorhabditis elegans. Aging Cell. 2015;14(1):92-101. Epub 2014/12/17. doi: 10.1111/acel.12301. PubMed PMID: 25510338; PubMed Central PMCID: PMCPMC4326909.

bioRxiv preprint doi: https://doi.org/10.1101/2023.05.05.539519; this version posted May 5, 2023. The copyright holder for this preprint (which was not certified by peer review) is the author/funder, who has granted bioRxiv a license to display the preprint in perpetuity. It is made available under aCC-BY 4.0 International license.

64. Iranon NN, Jochim BE, Miller DL. Fasting prevents hypoxia-induced defects of proteostasis in C. elegans. PLoS Genet. 2019;15(6):e1008242. Epub 2019/06/28. doi: 10.1371/journal.pgen.1008242. PubMed PMID: 31246952; PubMed Central PMCID: PMCPMC6619831.
65. Rechavi O, Houri-Ze'evi L, Anava S, Goh WSS, Kerk SY, Hannon GJ, et al. Starvation-induced transgenerational inheritance of small RNAs in C. elegans. Cell. 2014;158(2):277-87. Epub 2014/07/16. doi: 10.1016/j.cell.2014.06.020. PubMed PMID: 25018105; PubMed Central PMCID: PMCPMC4377509.
66. Vogt MC, Hobert O. Starvation-induced changes in somatic insulin/IGF-1R signaling drive metabolic programming across generations. Sci Adv. 2023;9(14):eade1817. Epub 2023/04/08. doi: 10.1126/sciadv.ade1817. PubMed PMID: 37027477; PubMed Central PMCID: PMCPMC10081852.
67. Wang SY, Kim K, O'Brown ZK, Levan A, Dodson AE, Kennedy SG, et al. Hypoxia induces transgenerational epigenetic inheritance of small RNAs. Cell Rep. 2022;41(11):111800. Epub 2022/12/15. doi: 10.1016/j.celrep.2022.111800. PubMed PMID: 36516753; PubMed Central PMCID: PMCPMC9847139.
68. Brenner S. The genetics of Caenorhabditis elegans. Genetics. 1974;77(1):71-94. Epub 1974/05/01. doi: 10.1093/genetics/77.1.71. PubMed PMID: 4366476; PubMed Central PMCID: PMCPMC1213120.
69. Hundley HA, Krauchuk AA, Bass BL. C. elegans and H. sapiens mRNAs with edited 3' UTRs are present on polysomes. RNA. 2008;14(10):2050-60. Epub 2008/08/23. doi: 10.1261/rna.1165008. PubMed PMID: 18719245; PubMed Central PMCID: PMCPMC2553745.
70. Thompson O, Edgley M, Strasbourger P, Flibotte S, Ewing B, Adair R, et al. The million mutation project: a new approach to genetics in Caenorhabditis elegans. Genome Res. 2013;23(10):1749-62. Epub 2013/06/27. doi: 10.1101/gr.157651.113. PubMed PMID: 23800452; PubMed Central PMCID: PMCPMC3787271.
71. Love MI, Huber W, Anders S. Moderated estimation of fold change and dispersion for RNA-seq data with DESeq2. Genome Biol. 2014;15(12):550. Epub 2014/12/18. doi: 10.1186/s13059-014-0550-8. PubMed PMID: 25516281; PubMed Central PMCID: PMCPMC4302049.

## Figure legends

**Figure 1- L1 animals lacking *adr-2* have decreased expression of genes regulated by insulin signaling.** (A) Volcano plot depicting gene expression in *adr-2(-)* neural cells compared to wildtype (WT) neural cells. Dots represent individual genes that are upregulated (red; 186, $p < 0.05$, log2fold > 0.5), downregulated (blue; 502, $p < 0.05$, log2fold < -0.5) or not significantly different (grey, $p \geq 0.05$) between three biological replicates of WT and *adr-2(-)* neural cells. (B-D) Expression of the indicated genes was determined relative to expression of the housekeeping gene *gpd-3*. Values were then normalized to wildtype neural cells (B) or wildtype L1 animals hatched in the absence of food (C, D) and the mean of three biological replicates was plotted. Error bars represent standard error of the mean (SEM). Statistical significance was calculated by two-way ANOVA test. **$p < 0.005$, ****$p < 0.0001$. ns indicates not significant ($p > 0.05$). For D, the indicated genotypes are of strains HAH30, HAH31, HAH32 and HAH33.

bioRxiv preprint doi: https://doi.org/10.1101/2023.05.05.539519; this version posted May 5, 2023. The copyright holder for this preprint (which was not certified by peer review) is the author/funder, who has granted bioRxiv a license to display the preprint in perpetuity. It is made available under aCC-BY 4.0 International license.

**Figure 2- Neural ADR-2 regulates insulin signaling cell non-autonomously in an editing independent manner.** (A, C) Gene expression of L1-arrested animals measured by qPCR. Expression of the indicated genes was determined relative to expression of the housekeeping gene *gpd-3*. Values were then normalized to WT and the mean of three (C) or four (A) biological replicates was plotted. Error bars represent standard error of the mean (SEM). Statistical significance was calculated by two-way ANOVA test. ****p < 0.0001, **p < 0.005, *p < 0.05 and ns indicates not significant (p > 0.05). For A, the indicated genotypes are of strains HAH23, HAH40 and HAH41. For C, the indicated genotypes are of strains N2, BB20 and HAH22 (B) A dashed line was used to outline the whole worm. For all the strains, the images are representative of 7-10 samples imaged in two biological replicates.

**Figure 3- Neural PQM-1 activity is sufficient to rescue expression of PQM-1 activated genes in *adr-2(-)* animals** (A-D) Gene expression of (A) neural cells and (B-D) L1-arrested animals measured by qPCR. Expression of indicated genes was determined relative to expression of the housekeeping gene gpd-3. Values were then normalized to WT and the mean of three biological replicates was plotted. Error bars represent standard error of the mean (SEM). Statistical significance was calculated by (A) multiple unpaired t tests and (B-D) two-way ANOVA test. ****p < 0.0001 and ns indicates not significant (p > 0.05). For A and B, the indicated genotypes are of strains HAH45 and HAH46. For C, the indicated genotypes are of strains HAH35, HAH37, HAH38 and HAH39. For D, the indicated genotypes are of strains HAH24, HAH41, HAH42, HAH43 and HAH44.

**Figure 4- Neural ADR-1 binding of *pqm-1* affects expression of PQM-1 activated genes.** (A,C) Gene expression of L1-arrested animals measured by qPCR. Expression of the indicated genes was determined relative to expression of the housekeeping gene *gpd-3*. Values were then normalized to WT and the mean of three biological replicates was plotted. Error bars represent standard error of the mean (SEM). Statistical significance was calculated by two-way ANOVA test. ***p < 0.0005, **p < 0.01, *p <0.05. For A, the indicated genotypes are of strains N2, BB19, BB20 and BB21. For C, the indicated genotypes are of strains HAH48, HAH49 and HAH50. (B) Western blot depicting immunoprecipitation of neural ADR-1 from the indicated strains. Bar graph represents the fold enrichment determined by dividing IP/Input value from qPCR for the indicated strains divided by that of negative control. Values were then normalized to negative control and the mean of three biological replicates was plotted. Error bars represent SEM. Statistical significance was calculated by multiple unpaired t tests. **p < 0.005.

**Figure 5- Survival of hatched L1 animals after CoCl2 exposure.** (A-B) Survival of transgenic (A) and non-transgenic (B) hatched L1 animals under hypoxic conditions induced by $CoCl_2$ exposure. Data plotted is average of three biological replicates. Error bars represent standard error of the mean (SEM).

bioRxiv preprint doi: https://doi.org/10.1101/2023.05.05.539519; this version posted May 5, 2023. The copyright holder for this preprint (which was not certified by peer review) is the author/funder, who has granted bioRxiv a license to display the preprint in perpetuity. It is made available under aCC-BY 4.0 International license.

**Supplemental Figure S1- Gene set enrichment analysis for genes with altered expression in *adr-2(-)* neural cells compared to wildtype neural cells.** For the total number of input genes in each of the categories (regulated gene set), the P value is calculated using Fisher's exact test. 'Count' indicates the number of genes within a specific category. The size and color of the circles for each of the categories signifies the number of genes (size) and P value (color) for the categories mentioned (see key in figure).

**Supplemental Figure S2- Overlap between datasets from Tepper et al, 2013 and genes misregulated in *adr-2(-)* neural cells.** DAF-16 activated (yellow circle) and PQM-1 activated (blue circle) genes from Tepper et al, 2013 were individually overlapped with the genes found to be upregulated (green circle) and downregulated (light red circle) genes in *adr-2(-)* neural cells compared to wildtype neural cells. The number in parentheses denotes the number of overlapped genes between the two datasets expected due to random chance.

**Supplemental Figure S3- L1 survival under hypoxic conditions. (**A-B) Survival of transgenic (A) and non- transgenic (B) hatched L1 animals with number of alive L1s on Y axis and varying concentrations of $CoCl_2$ on X axis. Error bars represent standard error of the mean (SEM). Statistical significance across strains was calculated using two-way ANOVA test. ****p < 0.0001

**Supplemental Figure S4- DAF-2 ligands downregulated in *adr-2(-)* neural cells.** Plot depicting expression of the 20 moderately expressed (read counts between 50-300) or highly expressed (read counts > 300) ILPs in *adr-2(-)* neural cells from the neural RNA sequencing dataset. Red dots indicate ligands that have significantly decreased expression in *adr-2(-)* neural cells compared to wildtype neural cells and are annotated. ILPs with p value < 0.05 and log2fold change <-0.5 were considered significantly downregulated.

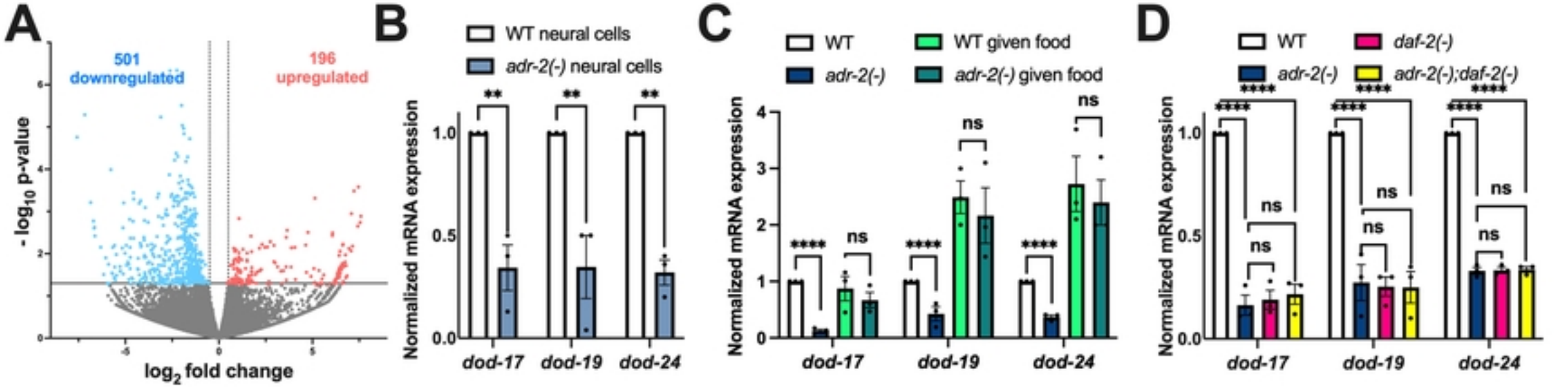
A
501
downregulated
196
upregulated
- log10 p-value
log2 fold change
B
WT neural cells
adr-2(-) neural cells
Normalized mRNA expression
dod-17
dod-19
dod-24
C
WT
adr-2(-)
WT given food
adr-2(-) given food
Normalized mRNA expression
ns
dod-17
dod-19
dod-24
D
WT
adr-2(-)
daf-2(-)
adr-2(-);daf-2(-)
Normalized mRNA expression
ns
dod-17
dod-19
dod-24

Figure 1

bioRxiv preprint doi: https://doi.org/10.1101/2023.05.05.539519; this version posted May 5, 2023. The copyright holder for this preprint (which was not certified by peer review) is the author/funder, who has granted bioRxiv a license to display the preprint in perpetuity. It is made available under a CC-BY 4.0 International license.

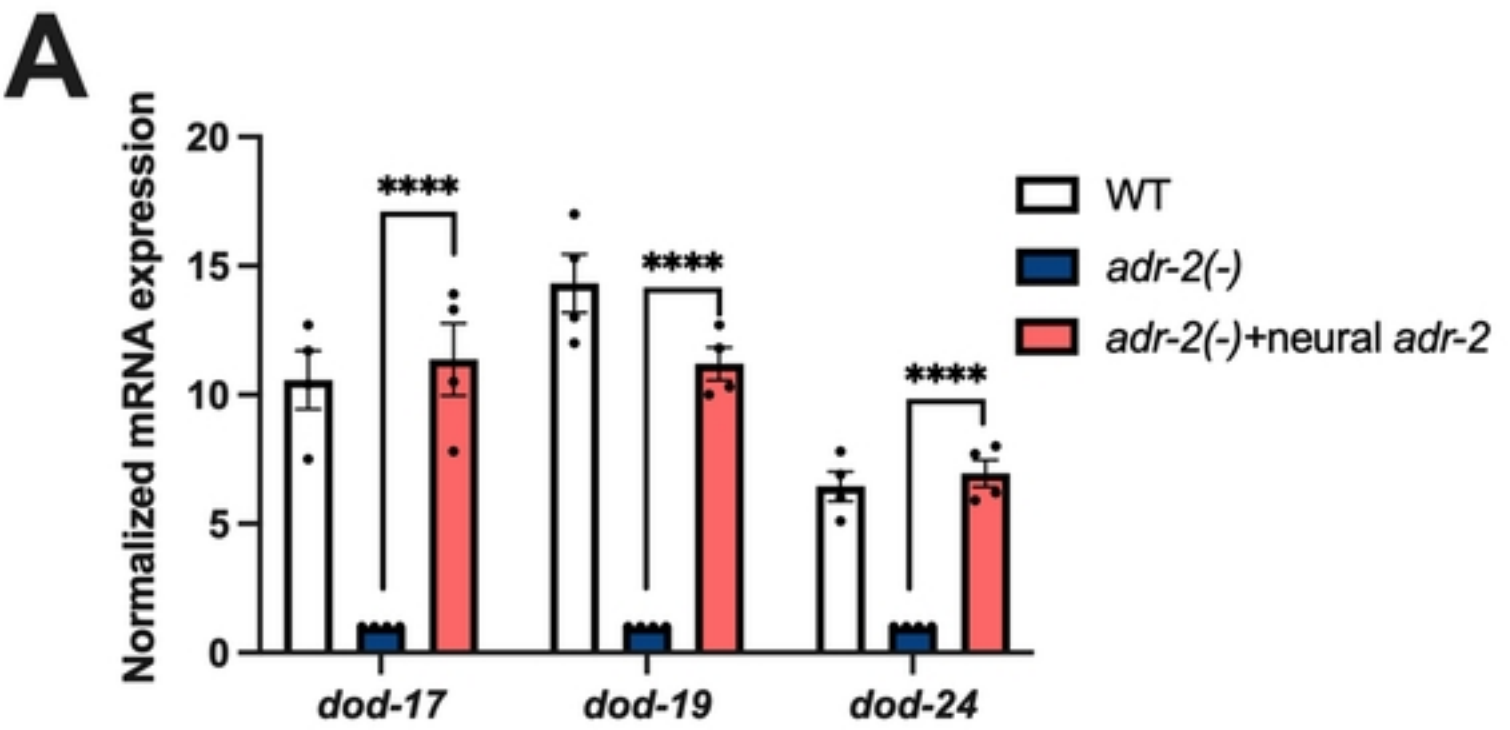



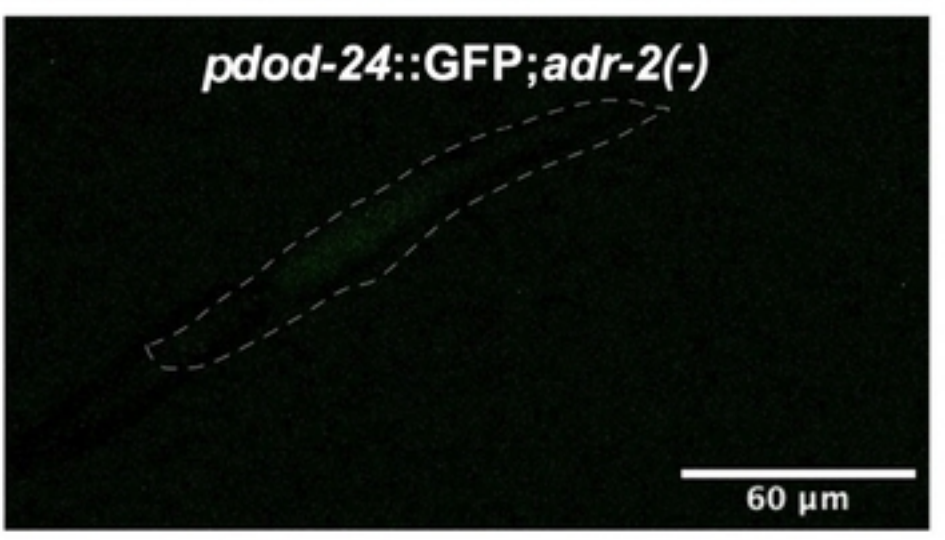


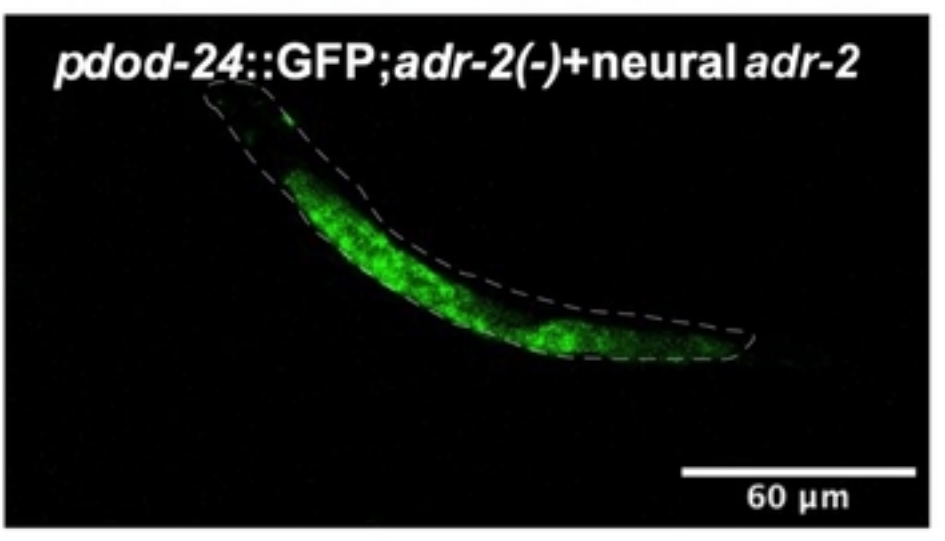


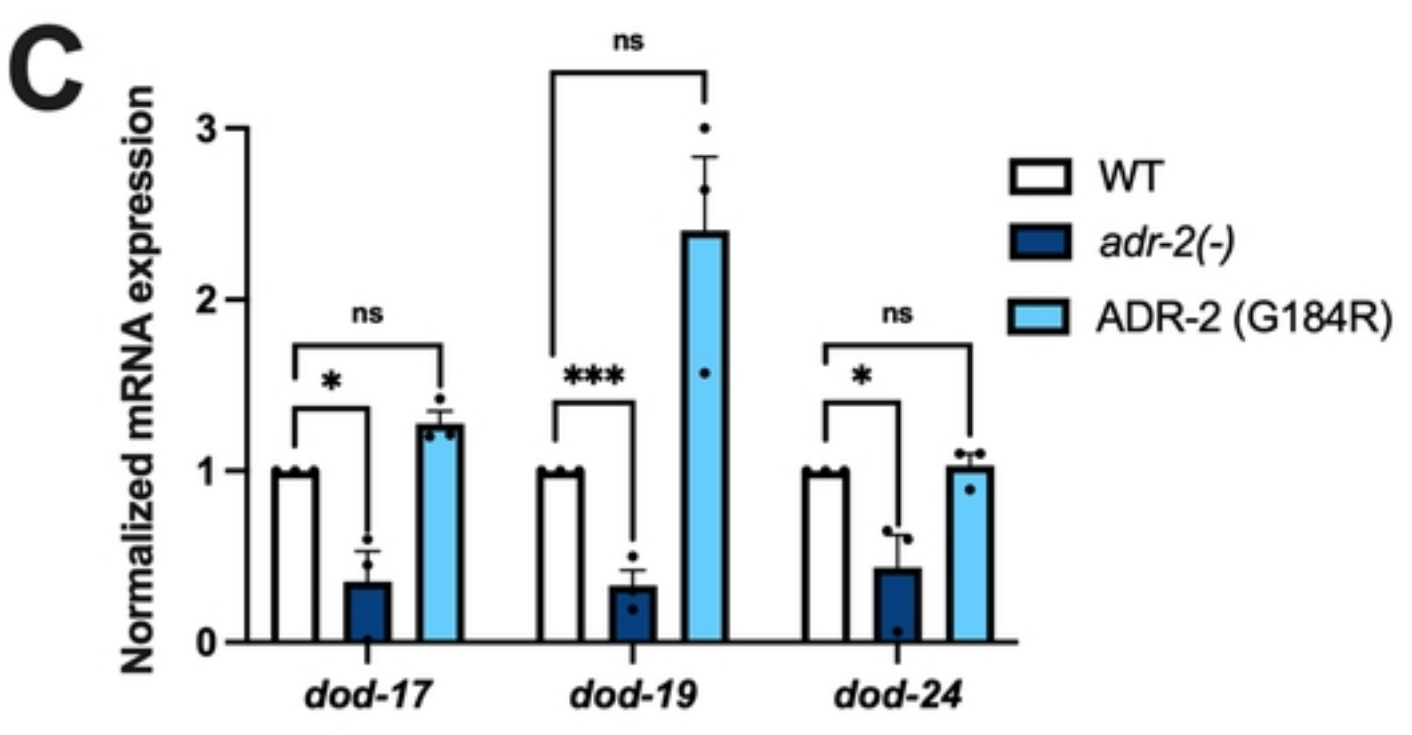


Figure 2

bioRxiv preprint doi: https://doi.org/10.1101/2023.05.05.539519; this version posted May 5, 2023. The copyright holder for this preprint (which was not certified by peer review) is the author/funder, who has granted bioRxiv a license to display the preprint in perpetuity. It is made available under aCC-BY 4.0 International license.

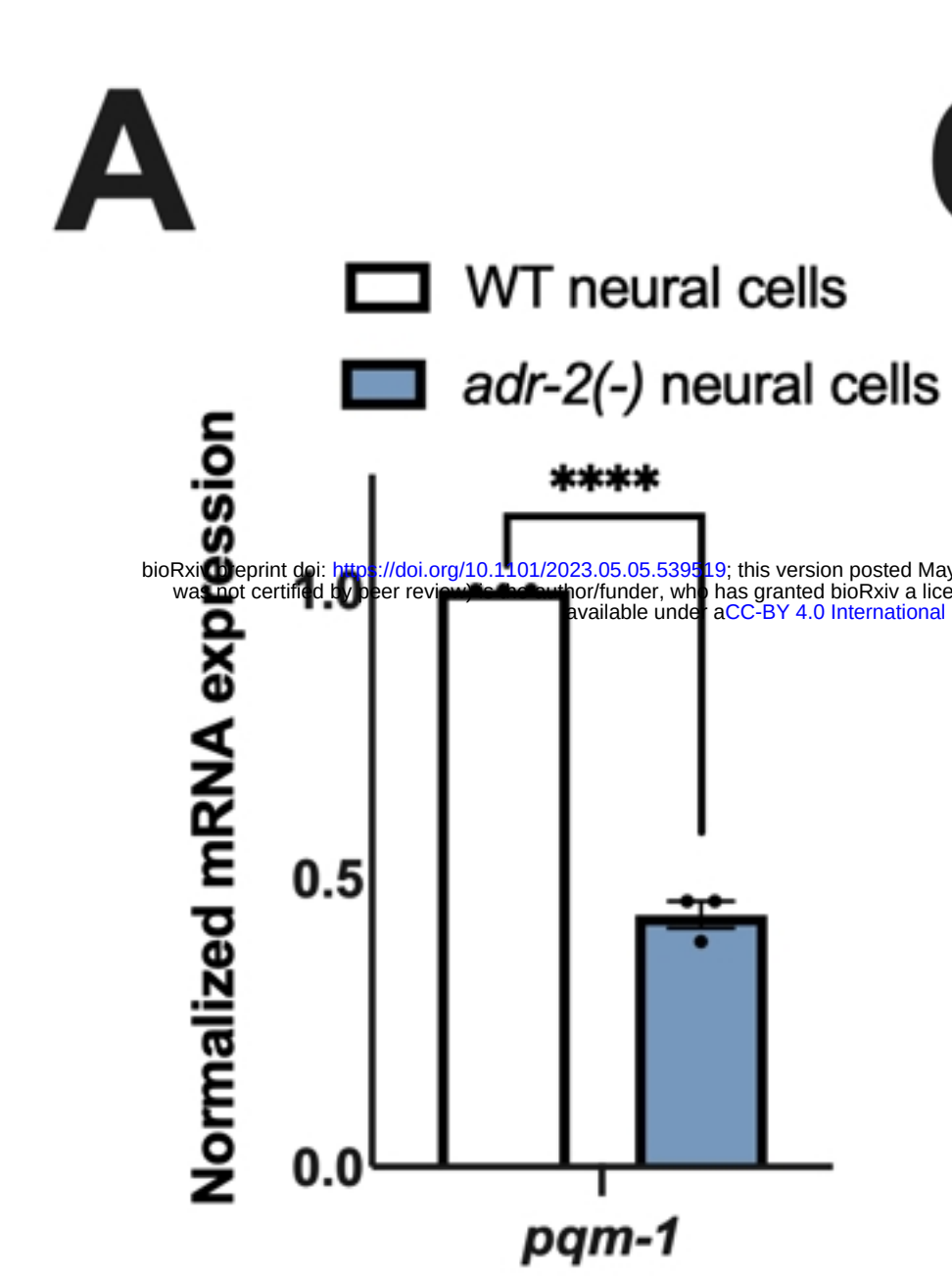


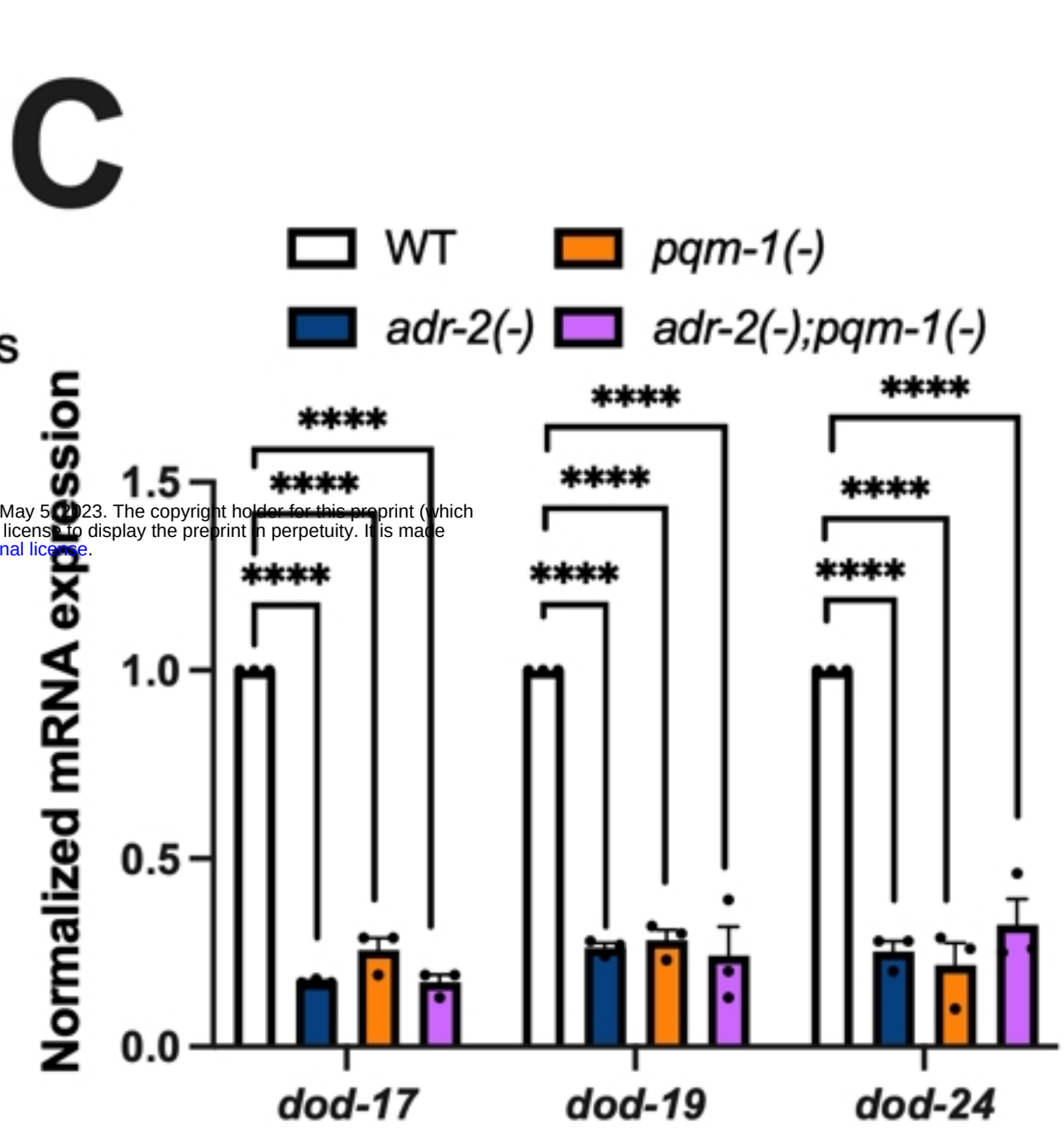


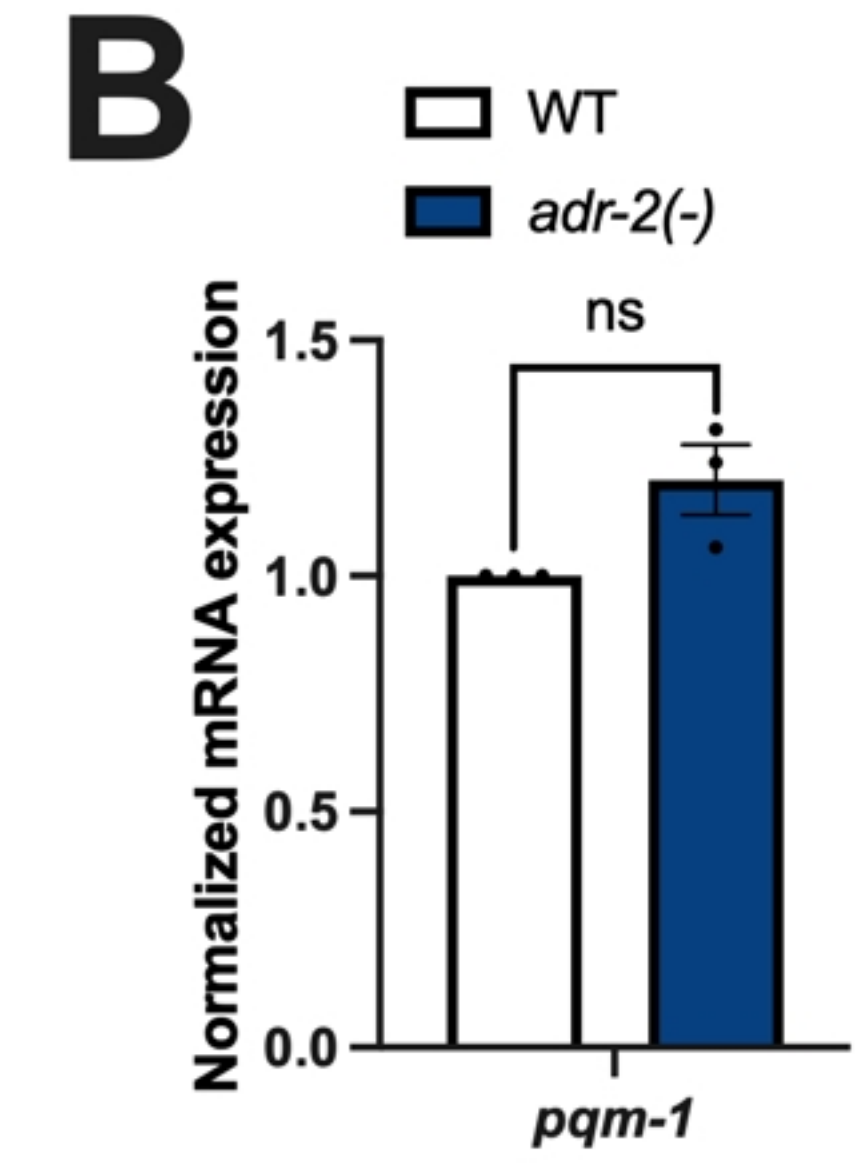


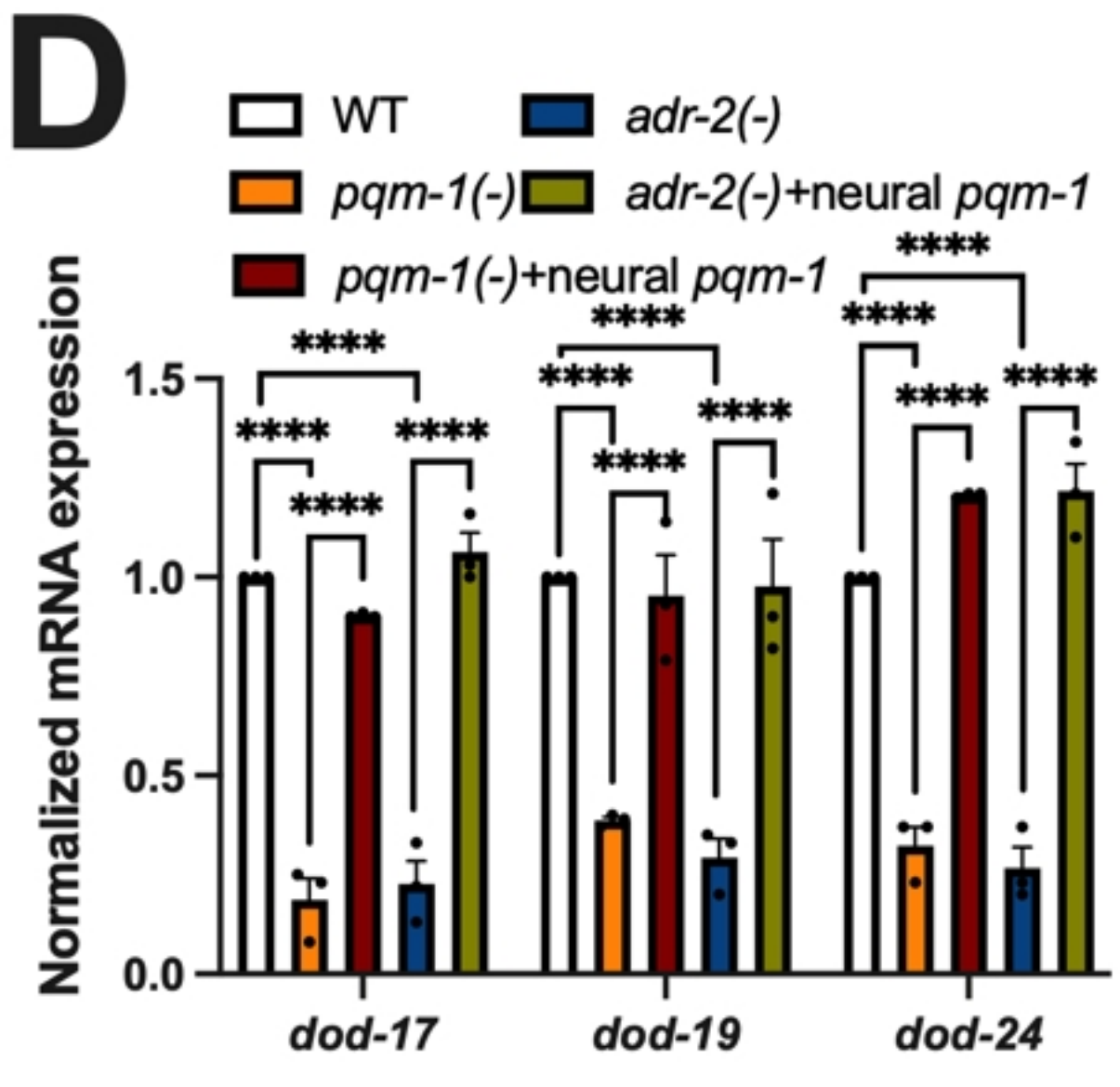


Figure 3

bioRxiv preprint doi: https://doi.org/10.1101/2023.05.05.539519; this version posted May 5, 2023. The copyright holder for this preprint (which was not certified by peer review) is the author/funder, who has granted bioRxiv a license to display the preprint in perpetuity. It is made available under aCC-BY 4.0 International license.

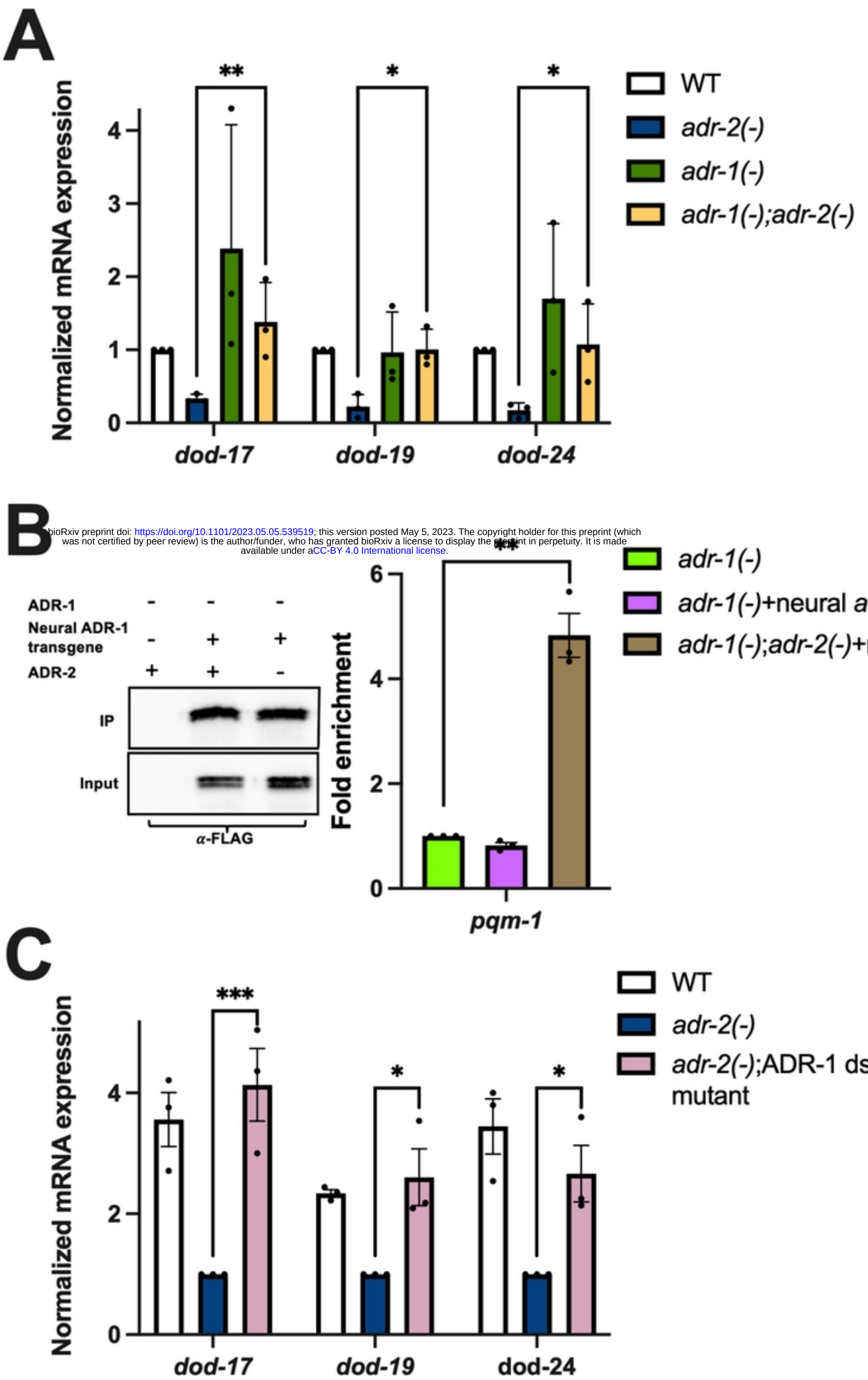


Figure 4

bioRxiv preprint doi: https://doi.org/10.1101/2023.05.05.539519; this version posted May 5, 2023. The copyright holder for this preprint (which was not certified by peer review) is the author/funder, who has granted bioRxiv a license to display the preprint in perpetuity. It is made available under aCC-BY 4.0 International license.

A

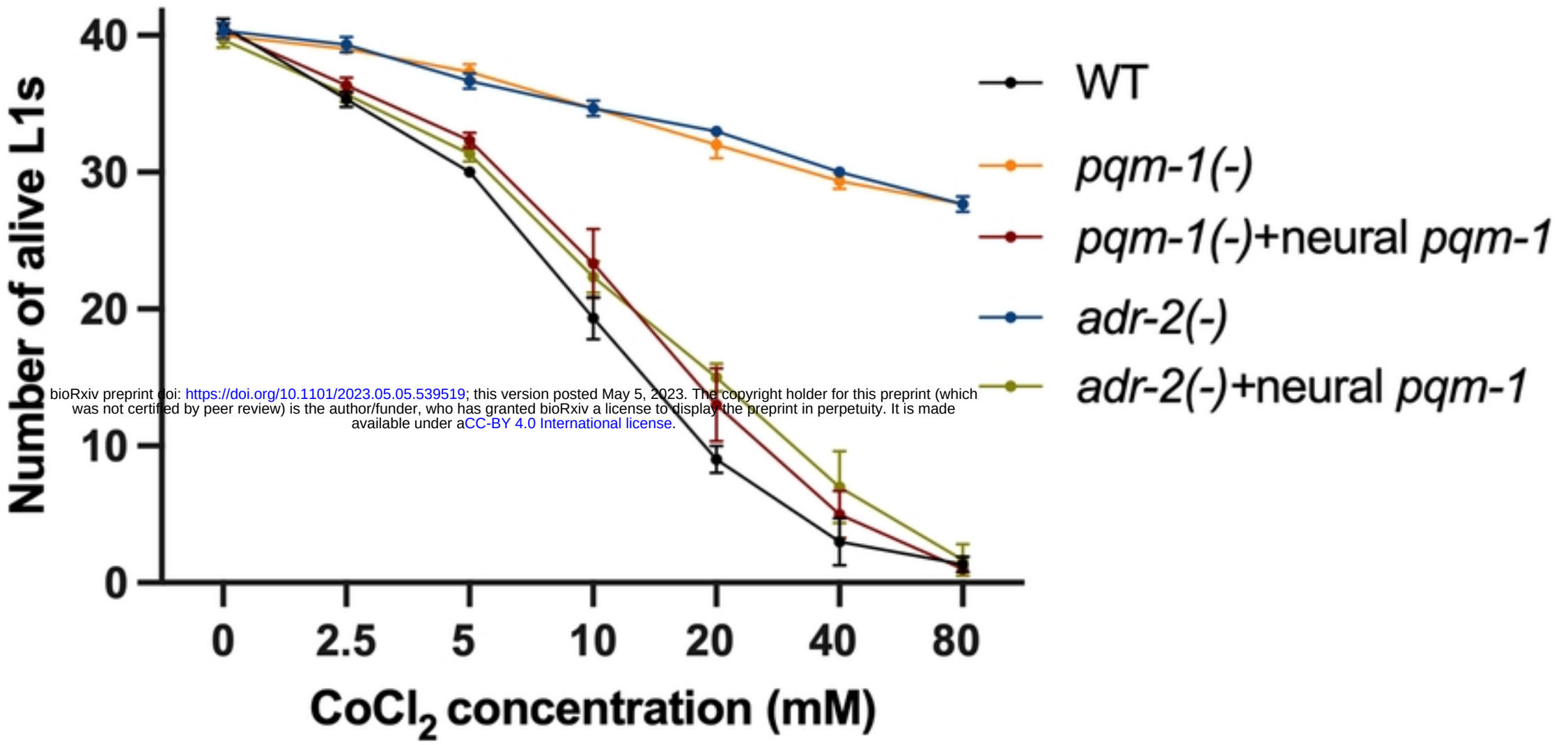


B

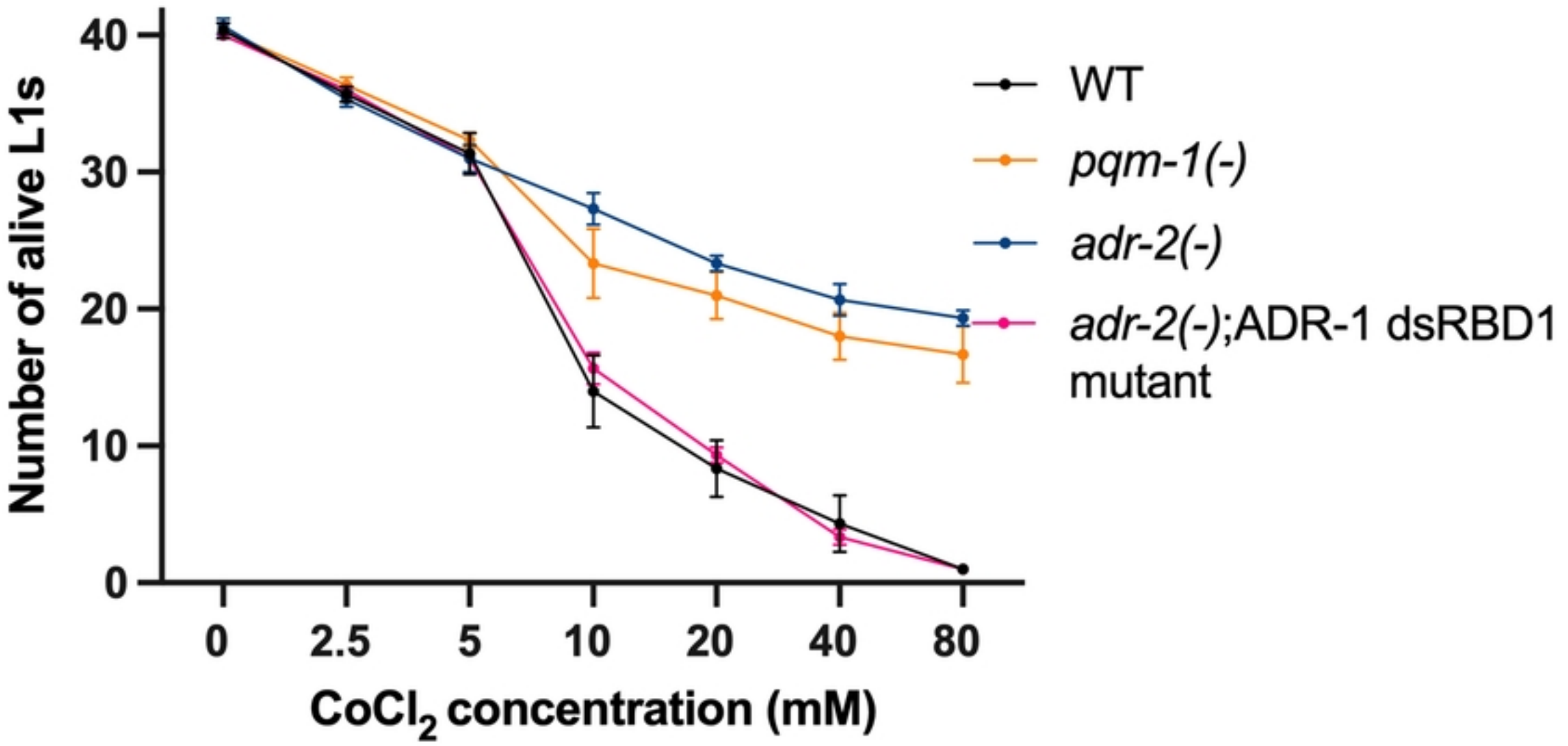


Figure 5